

MATHICSE Technical Report

Nr. 30 .2016

July 2016



Multiscale methods and model order reduction for flow problems in three-scale porous media

Assyr Abdulle, Ondrej Budáč, Antoine Imboden

Multiscale methods and model order reduction for flow problems in three-scale porous media

Assyr Abdulle*, Ondrej Budáč†, Antoine Imboden

Abstract

A new multiscale method combined with model order reduction is proposed for flow problems in three-scale porous media. We derive an effective three-scale model that couples a macroscopic Darcy equation, a mesoscopic Stokes–Brinkman equation, and a microscopic Stokes equation. A corresponding three-scale numerical method is then derived using the finite element discretization with numerical quadrature, where the macroscopic and mesoscopic permeability is upscaled at quadrature points from mesoscopic and microscopic problems, respectively. The computational cost of solving numerous mesoscopic and microscopic flow problems is further reduced by applying a Petrov–Galerkin reduced basis method at the mesoscopic and microscopic scales. As there is no natural way to obtain an affine decomposition of the mesoscopic problems, which is instrumental for the efficiency of the model order reduction, we derive a mesoscopic solver that makes use of empirical interpolation techniques. A priori and a posteriori error estimates are derived for the new method that is also tested numerically to corroborate the theoretical convergence rates and illustrate its efficiency.

Keywords. Stokes and Stokes–Brinkman flow, Darcy flow, three-scale porous media, numerical homogenization, reduced basis method

AMS subject classifications. 65N30, 76D07, 74Qxx, 35Q86

Introduction

Upscaling fluid flow in porous media is a basic problems in many applications in science and engineering. The oldest rigorous model based on observations was developed by Darcy [18]. In the current notation, the Darcy equation an elliptic *partial differential equation* (PDE) that describes effective velocity and pressure in a porous medium. The porous structure of the medium is hidden in the so-called effective permeability that is often modelled empirically. This can however be difficult in some situations, especially for new materials or when experiments are infeasible. This permeability can be obtained from more fundamental principle, namely by considering the porous structure of the material and the Stokes equation in a domain decomposed into fluid and solid parts. The Stokes model is justified as the Reynolds number is usually small in such flow problems. In practice, using meshing-based numerical techniques to solve this Stokes problem is often infeasible due to the enormous number of *degrees of freedom* (DOF) required to represent the complicated micro-structure of the porous media.

The effective Darcy model and the fine-scale Stokes model can be bridged by homogenization theory, which studies asymptotic properties of the fine-scale Stokes model when the characteristic size of the porous structure goes to zero. Rigorous results are available for periodic porous media [6, 27, 28], locally periodic porous media [12], and random porous media [10]. The limit problem is indeed a Darcy equation, whose effective permeability at any point is linked to the local porous structure. The so-called Stokes micro problems can

*ANMC, Section de Mathématiques, École polytechnique fédérale de Lausanne, 1015 Lausanne, Switzerland, Assyr.Abdulle@epfl.ch

†ANMC, Section de Mathématiques, École polytechnique fédérale de Lausanne, 1015 Lausanne, Switzerland, Ondrej.Budac@epfl.ch

be solved in a small domain representing the local porous structure and the effective permeability can be obtained by averaging the velocity solutions. This two-scale model problem leads to numerical homogenization strategies to solve the Stokes flow in porous media. A numerical method is used to solve the effective Darcy problem, while the effective permeability is (approximately) upscaled at selected points (e.g., quadrature points of a finite element method) from numerical solutions of Stokes micro problems. We briefly mention a few of these methods. A control volume method is applied at the macro scale in [7]. The numerical multiscale method in [12] uses a *finite element method* (FEM) with a hierarchy of macroscopic grids where micro problems are solved with various accuracy. The *Darcy-Stokes finite element heterogeneous multiscale method* (DS-FE-HMM) that has been introduced in [1] uses FEM to discretize both scales.

In the present work we are interested in porous media that do not fit into the two-scale framework because they contain porous structures of several incommensurate scales. If a two-scale numerical method is applied to such media, the Stokes micro problems will be solved in micro domains that are again porous, at some smaller scale. Thus, the complexity of the micro domains can be too large, yielding a prohibitive number of DOF at the micro scale. A periodic three-scale (macro, meso, and micro scale) porous medium and homogenization of Stokes flow in such medium has been derived in [19]. The model couples a macroscopic Darcy equation whose permeability is upscaled by averaging the velocities from mesoscopic problems modelled by the Stokes–Brinkman equation. These meso problems are defined in domains in which the medium is divided into a fluid and a porous part. Finally the mesoscopic permeability in the porous part is upscaled by averaging the velocities from Stokes micro problems. This model is discussed in [19] and numerical experiments related to textile models have been presented. However, the numerical method makes use of precomputed empirically derived parameters to avoid the discretisation and the coupling of the three distinct scales.

In this paper we present the first multiscale method based on simultaneous discretisation of a three-scale problem in porous media. The method is based on numerical homogenization and is computationally feasible thanks to model order reduction techniques blended into the computational strategy. We first extend the framework of the heterogeneous multiscale method (HMM) introduced in [1] for three-scale problems. Finite element method with numerical quadrature is used to solve the macroscopic Darcy equation, where the effective macroscopic permeability is upscaled from mesoscopic computations at each macroscopic quadrature point. At the meso scale we use a stable FE scheme (Taylor–Hood FE) with numerical quadrature to solve the Stokes–Brinkman equation, where the effective mesoscopic permeability is upscaled from micro problems at every quadrature point in the porous subdomain. At the micro scale we use a stable FE scheme (Taylor–Hood FE) to solve the Stokes micro problems. The a priori error analysis confirms that to avoid error saturation, macro, meso, and micro meshes should be refined simultaneously, which limits the applicability of the method due to its large computational cost. We thus propose a model-order reduction on micro and meso scale to speed up the three-scale method. The *reduced basis* (RB) method is used at the micro scale, similarly to [4]. At the meso scale we cannot use the RB method directly since an affine decomposition of the reaction term is not available. To overcome this issue we introduce a new coupling that makes use of *empirical interpolation method* (EIM) and permits to employ reduced basis techniques simultaneously at the micro and at the meso scales. A priori error analysis illustrates the different contributions to the error of the multiscale scheme, namely the macro, meso, and micro mesh sizes, the RB size at the micro and meso scale, and the size of the EIM interpolation. A posteriori error analysis is also conducted, allowing for an adaptive macroscopic mesh refinement.

This paper is structured as follows. In section 1 we describe two-scale and three-scale porous media and derive the three-scale model problem in section 2, which is discretized using the finite element method in section 3. We recall the Petrov–Galerkin reduced basis method for non-coercive problems in section 4. In section 5 we apply this RB method to the three-scale numerical method and derive and analyze a new reduced basis three-scale numerical method for Stokes flow in porous media. Numerical experiments that corroborate the analysis and illustrate the efficiency of the numerical method are detailed in section 6.

Notation. Let C denote a generic constant whose value can change at any occurrence but it depends only on explicitly indicated quantities. We consider a domain $\Omega \subset \mathbb{R}^d$, $d \in \{2, 3\}$ and the usual Lebesgue space $L^p(\Omega)$ and Sobolev space $W^{k,p}(\Omega)$ equipped with the usual norms $\|\cdot\|_{L^p(\Omega)}$ and $\|\cdot\|_{W^{k,p}(\Omega)}$. For $p = 2$ we apply the Hilbert space notation $H^k(\Omega)$ and $H_0^1(\Omega)$ and define the seminorm $|q|_{H^1(\Omega)} = (\sum_{i=1}^d \|\partial_i q\|_{L^2(\Omega)}^2)^{1/2}$. Given a matrix $A = (a_{ij})_{1 \leq i, j \leq d} \in \mathbb{R}^{d \times d}$ we denote its Frobenius norm by $\|A\|_F = (\sum_{i,j=1}^d a_{ij}^2)^{1/2}$. Given a vector $\xi = (\xi_1, \dots, \xi_d)^\top \in \mathbb{R}^d$ we define $|\xi| = (\sum_{i=1}^d \xi_i^2)^{1/2}$.

1 Multiscale porous media and homogenization

Let $d \in \{2, 3\}$ and $\Omega \subset \mathbb{R}^d$ be a connected bounded domain that contains solid and fluid part. We consider a porous medium in Ω that is given by the fluid subset $\Omega_\varepsilon \subset \Omega$, where $\varepsilon > 0$ denotes the characteristic scale of the porous structure. The domain Ω_ε is obtained from Ω by removing its solid part. Fluid flow in Ω_ε can be modeled by the Stokes problem: Find the velocity field \mathbf{u}^ε and the pressure p^ε such that

$$\begin{aligned} -\Delta \mathbf{u}^\varepsilon + \nabla p^\varepsilon &= \mathbf{f} & \text{in } \Omega_\varepsilon, \\ \operatorname{div} \mathbf{u}^\varepsilon &= 0 & \text{in } \Omega_\varepsilon, \\ \mathbf{u}^\varepsilon &= 0 & \text{on } \partial\Omega_\varepsilon, \end{aligned} \tag{1}$$

where \mathbf{f} is a given force field. Numerical approximations of (1) that are based on meshing of Ω_ε can be prohibitive even on modern supercomputers since the number of degrees of freedom scales with $\operatorname{volume}(\Omega)/\varepsilon^d$. We thus investigate an approximate model that was first introduced by Darcy [18] and was later obtained rigorously through the homogenization theory as an effective limit problem of (1). If Ω_ε is a periodic porous medium [6, 27, 28] or a locally periodic porous medium [13], the following limit behavior of $(\mathbf{u}^\varepsilon, p^\varepsilon)$ has been shown. The solution $(\mathbf{u}^\varepsilon, p^\varepsilon)$ can be extended from Ω_ε to Ω and denoted by $(\mathbf{U}^\varepsilon, P^\varepsilon)$ and we have $P^\varepsilon \rightarrow p^0$ strongly in $L^2_{\text{loc}}(\Omega)/\mathbb{R}$ and $\mathbf{U}^\varepsilon/\varepsilon^2 \rightarrow \mathbf{u}^0$ weakly in $L^2(\Omega)$, where p^0 and \mathbf{u}^0 are the homogenized pressure and the homogenized velocity, respectively. Moreover, p^0 is the solution to the effective Darcy problem

$$\begin{aligned} \nabla \cdot a^0(\mathbf{f} - \nabla p^0) &= 0 & \text{in } \Omega, \\ a^0(\mathbf{f} - \nabla p^0) \cdot \mathbf{n} &= 0 & \text{on } \partial\Omega, \end{aligned} \tag{2}$$

where the effective permeability a^0 can be upscaled from the porous structure of Ω_ε (described below) and $\mathbf{u}^0 = a^0(\mathbf{f} - \nabla p^0)$.

We briefly describe two-scale porous media and the two-scale model problem in section 1.1. However, the focus of this paper will be on porous media that have porous structures of incommensurate characteristic sizes. Such media can be described in the two-scale fashion but a resulting numerical two-scale method can be again prohibitive. We propose a definition of three-scale porous media and a three-scale effective model in section 1.2.

1.1. Two-scale model. Denote by Y the d -dimensional unit cube $(-1/2, 1/2)^d$, let $Y_S \subset \bar{Y}$, and set $Y_F = Y \setminus Y_S$. Here and subsequently the subscripts F and S stand for the fluid and solid part, respectively. Consider a continuous map $\varphi : \Omega \times \bar{Y} \rightarrow \bar{Y}$ such that for every $x \in \Omega$ the map $\varphi(x, \cdot) : \bar{Y} \rightarrow \bar{Y}$ is a homeomorphism. For any $x \in \Omega$ we define the local porous geometry (Y_S^x, Y_F^x) by $Y_S^x = \varphi(x, Y_S)$ and $Y_F^x = Y \setminus Y_S^x$. We then define a two-scale porous medium by

$$\Omega_\varepsilon = \Omega \setminus \cup_{k \in \mathbb{Z}^d} \varepsilon(k + Y_S^{\varepsilon k}). \tag{3}$$

For an example of this construction see Figure 1.

Remark 1. To apply definition (3) we need to extend φ to the domain $\mathbb{R}^d \times \bar{Y}$. If this extension is not given, one can use $\varphi(x, y) \equiv y$ for every $x \in \mathbb{R}^d \setminus \Omega$ by default. This only affects Ω_ε close to $\partial\Omega$.

We introduce some minimal regularity assumptions that allow the homogenization theory to be obtained (see [6]).

Assumption 2. We say that the porous geometry (Y_S, Y_F) satisfies the basic assumptions of the homogenization theory if:

- (i) the set Y_S is closed and both Y_S and Y_F have positive measure,
- (ii) the sets Y_F and $\mathbb{R}^d \setminus \cup_{k \in \mathbb{Z}^d} (k + Y_S)$ have locally Lipschitz boundaries and are locally located on one side of their boundaries,
- (iii) the sets Y_F and $\mathbb{R}^d \setminus \cup_{k \in \mathbb{Z}^d} (k + Y_S)$ are connected.

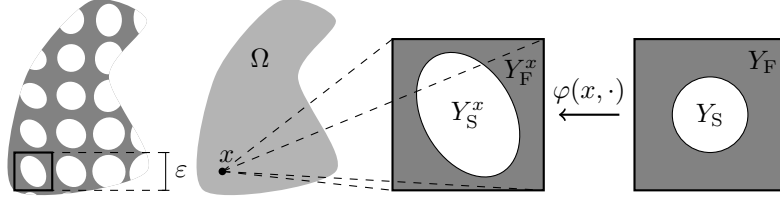


Figure 1: An example of the two-scale porous media Ω_ε . Here we did not use the default extension from Remark 1 since we considered $\varphi : \mathbb{R}^d \times \bar{Y} \rightarrow \bar{Y}$ from the beginning.

Effective permeability. For any point $x \in \Omega$ we compute the effective permeability $a^0(x)$ using the Stokes micro problems: For every $i \in \{1, \dots, d\}$ find the velocity $\mathbf{u}^{i,x}$ and pressure $p^{i,x}$ such that

$$\begin{aligned} -\Delta \mathbf{u}^{i,x} + \nabla p^{i,x} &= \mathbf{e}^i & \text{in } Y_F^x, & & \mathbf{u}^{i,x} &= 0 & \text{on } \partial Y_S^x, \\ \operatorname{div} \mathbf{u}^{i,x} &= 0 & \text{in } Y_F^x, & & \mathbf{u}^{i,x} \text{ and } p^{i,x} & \text{are } Y\text{-periodic,} \end{aligned} \quad (4)$$

where \mathbf{e}^i is the i -th canonical basis vector in \mathbb{R}^d . We then define $a_{ij}^0(x) = \int_{Y_F^x} \mathbf{e}^i \cdot \mathbf{u}^{j,x} dy$ for every $i, j \in \{1, \dots, d\}$. The tensor $a^0(x)$ is generally unknown and in practice it can be only obtained by a numerical approximation of (4).

1.2. Three-scale model. Let $d \in \{2, 3\}$ and $\Omega \subset \mathbb{R}^d$ be a connected bounded domain. We will define a porous medium $\Omega_{\varepsilon_1, \varepsilon_2} \subset \Omega$ with porous structures of characteristic sizes $\varepsilon_1, \varepsilon_2$, where $\varepsilon_1 \gg \varepsilon_2 > 0$. The scales corresponding to ε_1 and ε_2 are called the mesoscopic and the microscopic scale, respectively. We assume that ε_1 and ε_2 are positive functions of $\varepsilon \in \mathbb{R}^+$ such that $\lim_{\varepsilon \rightarrow 0} \varepsilon_1(\varepsilon) = 0$ and the micro scale is well-separated, a. e., $\lim_{\varepsilon \rightarrow 0} \varepsilon_2(\varepsilon)/\varepsilon_1(\varepsilon) = 0$. For an illustration of the construction that follows see Figure 2.

At the mesoscopic scale we consider two different regimes: fluid and porous (for a generalization see Remark 3). Let (Y_P, Y_F) be the reference mesoscopic geometry, where $Y_P \subset \bar{Y}$ represents the porous part and $Y_F = \bar{Y} \setminus Y_P$ represents the fluid part. We suppose that (Y_P, Y_F) satisfies Assumption 2(i) and (ii). Consider a continuous map $\varphi_{\text{mes}} : \Omega \times \bar{Y} \rightarrow \bar{Y}$ such that $\varphi_{\text{mes}}(x, \cdot) : \bar{Y} \rightarrow \bar{Y}$ is a homeomorphism for every $x \in \Omega$. We suppose that $\varphi_{\text{mes}}(x, \cdot), \varphi_{\text{mes}}(x, \cdot)^{-1} \in W^{1, \infty}(Y)^d$ for every $x \in \Omega$ and that there is a constant Λ_φ such that

$$\|\varphi_{\text{mes}}(x, \cdot)\|_{W^{1, \infty}(Y)^d} \leq \Lambda_\varphi, \quad \|\varphi_{\text{mes}}(x, \cdot)^{-1}\|_{W^{1, \infty}(Y)^d} \leq \Lambda_\varphi, \quad \forall x \in \Omega. \quad (5)$$

For any $x \in \Omega$ we define the local mesoscopic geometry by $Y_P^x = \varphi_{\text{mes}}(x, Y_P)$ and $Y_F^x = \varphi_{\text{mes}}(x, Y_F)$. The porous structure in Y_P^x can be described in detail by considering the micro scale features.

Remark 3. It is possible to consider three regimes at the meso scale: porous, fluid, and solid. Since this generalization is straightforward but makes the analysis more technical, we prefer the simpler model that we introduced.

At the microscopic scale we distinguish two regimes of the material: fluid and solid. Let $Z = (-0.5, 0.5)^d$ be the microscopic unit cube¹ and let (Z_S, Z_F) be the reference microscopic

¹Technically Y and Z are identical but we use different notation to clearly distinguish between mesoscopic and microscopic objects. Also, notice the difference between the unit cube Z and the set of integers \mathbb{Z} .

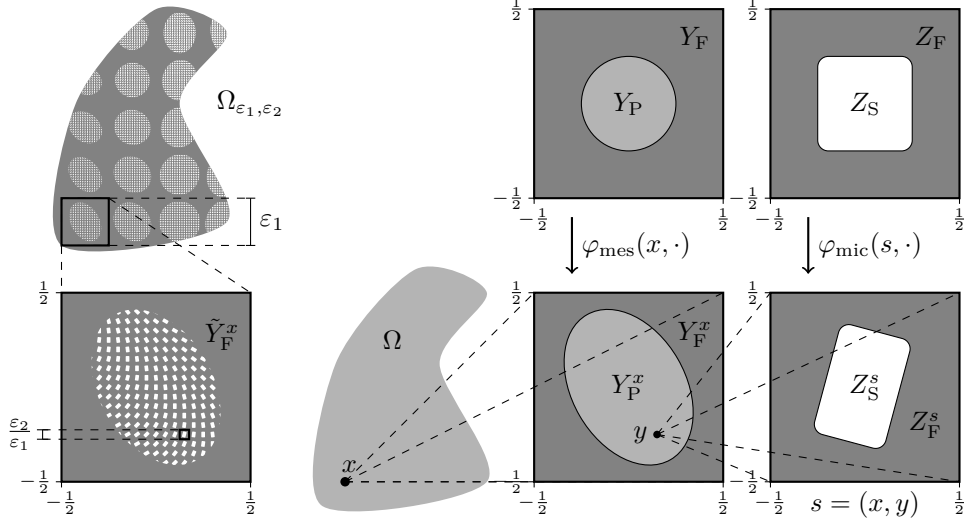


Figure 2: The construction of a three-scale porous medium $\Omega_{\varepsilon_1, \varepsilon_2}$.

geometry, where $Z_S \subset \bar{Z}$ and $Z_F = Z \setminus Z_S$. We suppose that (Z_S, Z_F) satisfies Assumption 2. Let $\varphi_{\text{mic}} : \Omega \times Y \times \bar{Z} \rightarrow \bar{Z}$ be such that $\varphi_{\text{mic}}(x, y, \cdot) : \bar{Z} \rightarrow \bar{Z}$ is a homeomorphism for every $(x, y) \in \Omega \times Y$. We suppose that $\varphi_{\text{mic}}(x, y, \cdot), \varphi_{\text{mes}}(x, y, \cdot)^{-1} \in W^{1, \infty}(Z)^d$ for every $x \in \Omega$ and $y \in Y$ and that there is a constant Λ_φ such that

$$\|\varphi_{\text{mic}}(x, y, \cdot)\|_{W^{1, \infty}(Z)^d} \leq \Lambda_\varphi, \quad \|\varphi_{\text{mic}}(x, y, \cdot)^{-1}\|_{W^{1, \infty}(Z)^d} \leq \Lambda_\varphi, \quad \forall (x, y) \in \Omega \times Y. \quad (6)$$

Since we often fix coordinates $x \in \Omega$ and $y \in Y$ to represent a microscopic location, we simplify the notation by denoting this pair as $s = (x, y)$. Hence, we can write $\varphi_{\text{mic}}(x, y, z) \equiv \varphi_{\text{mic}}(s, z)$. For any $s \in \Omega \times Y$ we define the local microscopic geometry as $Z_S^s = \varphi_{\text{mic}}(s, Z_S)$ and $Z_F^s = \varphi_{\text{mic}}(s, Z_F)$.

For any $x \in \Omega$ we consider the local mesoscopic geometry (Y_F^x, Y_P^x) , where the porous part Y_P^x is further decomposed using the microscopic porous structure. The mesoscopic domain is thus split into a solid part \tilde{Y}_S^x and a fluid part \tilde{Y}_F^x , where $Y_F^x \subset \tilde{Y}_F^x$ and $\tilde{Y}_S^x \subset Y_P^x$. Let

$$\tilde{Y}_S^x = Y_P^x \setminus \bigcup_{k \in \mathbb{Z}^d} \frac{\varepsilon_2}{\varepsilon_1} (k + Z_S^{\frac{\varepsilon_2}{\varepsilon_1} k}), \quad \tilde{Y}_F^x = Y \setminus \tilde{Y}_S^x. \quad (7)$$

We next define the fine scale structure of the three-scale porous medium in Ω by

$$\Omega_{\varepsilon_1, \varepsilon_2} = \Omega \setminus \bigcup_{k \in \mathbb{Z}^d} \varepsilon_1 (k + \tilde{Y}_S^{\varepsilon_1 k}). \quad (8)$$

Notice that in (7) and (8) the functions φ_{mes} and φ_{mic} are used outside their domain of definition. We resolve this discrepancy using the same approach as in Remark 1.

1.3. Formal homogenization. We discuss here a fluid flow in a three-scale porous medium and derive an effective three-scale model, which is summarized in Table 1. One could model a fluid flow in $\Omega_{\varepsilon_1, \varepsilon_2}$ using the Stokes equation as in (1): find the velocity field $\mathbf{u}^{\varepsilon_1, \varepsilon_2}$ and pressure $p^{\varepsilon_1, \varepsilon_2}$ such that

$$\begin{aligned} -\Delta \mathbf{u}^{\varepsilon_1, \varepsilon_2} + \nabla p^{\varepsilon_1, \varepsilon_2} &= \mathbf{f} & \text{in } \Omega_{\varepsilon_1, \varepsilon_2}, \\ \operatorname{div} \mathbf{u}^{\varepsilon_1, \varepsilon_2} &= 0 & \text{in } \Omega_{\varepsilon_1, \varepsilon_2}, \\ \mathbf{u}^{\varepsilon_1, \varepsilon_2} &= 0 & \text{on } \partial \Omega_{\varepsilon_1, \varepsilon_2}. \end{aligned} \quad (9)$$

The complexity of $\Omega_{\varepsilon_1, \varepsilon_2}$ makes a direct numerical approximation of (9) prohibitive. If we apply the two-scale effective problem framework in the three-scale media we would obtain the macroscopic Darcy equation (2) at the macro scale and the following microscopic

Stokes equation. For any $x \in \Omega$ and $i \in \{1, \dots, d\}$ find the velocity field $\tilde{\mathbf{u}}^{i,x}$ and the pressure $\tilde{p}^{i,x}$ such that

$$\begin{aligned} -\Delta \tilde{\mathbf{u}}^{i,x} + \nabla \tilde{p}^{i,x} &= \mathbf{e}^i & \text{in } \tilde{Y}_{\mathbb{F}}^x, & & \tilde{\mathbf{u}}^{i,x} &= 0 & \text{on } \partial \tilde{Y}_{\mathbb{S}}^x, \\ \operatorname{div} \tilde{\mathbf{u}}^{i,x} &= 0 & \text{in } \tilde{Y}_{\mathbb{F}}^x, & & \tilde{\mathbf{u}}^{i,x} \text{ and } \tilde{p}^{i,x} & \text{are } Y\text{-periodic.} \end{aligned} \quad (10)$$

The computational domain $\tilde{Y}_{\mathbb{F}}^x$ defined in (7) contains porous structures of characteristic scale $\varepsilon_2/\varepsilon_1$. Hence, meshing of $\tilde{Y}_{\mathbb{F}}^x$ and a direct numerical approximation of (10) can be again prohibitive. We solve this problem by applying homogenization theory again. We approximate the Stokes model in $\tilde{Y}_{\mathbb{F}}^x$ by a Darcy model in $Y_{\mathbb{P}}^x$ and a Stokes model in $Y_{\mathbb{F}}^x$. The effective permeability of the Darcy flow in $Y_{\mathbb{P}}^x$ can be upscaled from microscopic problems in domains $Z_{\mathbb{F}}^{x,y}$. This leads to a different mesoscopic problem: for any $i \in \{1, \dots, d\}$ and $x \in \Omega$ find the velocity field $\mathbf{u}^{i,x}$ and the pressure $p^{i,x}$ such that

$$\begin{aligned} -\Delta \mathbf{u}^{i,x} + \nabla p^{i,x} &= \mathbf{e}^i & \text{in } Y_{\mathbb{F}}^x, & & \operatorname{div} \mathbf{u}^{i,x} &= 0 & \text{in } Y, \\ \frac{\varepsilon_2^2}{\varepsilon_1^2} b^0(\mathbf{e}^i - \nabla p^{i,x}) &= \mathbf{u}^{i,x} & \text{in } Y_{\mathbb{P}}^x, & & \mathbf{u}^{i,x} \text{ and } p^{i,x} & \text{are } Y\text{-periodic,} \end{aligned} \quad (11)$$

where b^0 is the mesoscopic permeability defined below. Note that the problem (11) is incomplete since we have not specified coupling of the Stokes and Darcy problem over their interface $\partial Y_{\mathbb{P}}^x$. This coupling has been studied extensively and a standard approach is to use the Beavers–Joesph–Saffman interface conditions [9, 21, 26]. We use a simpler approach that is well justified for $\varepsilon_2/\varepsilon_1 \ll 1$, see [19]. We replace the Darcy model in $Y_{\mathbb{P}}^x$ by the Brinkman model, which allows for a simple interface conditions requiring only continuity of $\mathbf{u}^{i,x}$ and $p^{i,x}$ over $\partial Y_{\mathbb{P}}^x$. Hence, we introduce the mesoscopic Stokes–Brinkman model: for any $i \in \{1, \dots, d\}$ and $x \in \Omega$ find the velocity $\mathbf{u}^{i,x}$ and pressure $p^{i,x}$ such that

$$\begin{aligned} -\Delta \mathbf{u}^{i,x} + \nabla p^{i,x} + K^0 \mathbf{u}^{i,x} &= \mathbf{e}^i & \text{in } Y, & & \mathbf{u}^{i,x}, p^{i,x} & \text{are } Y\text{-periodic,} \\ \operatorname{div} \mathbf{u}^{i,x} &= 0 & \text{in } Y, & & & \end{aligned} \quad (12)$$

where

$$K^0(x, y) = \begin{cases} \frac{\varepsilon_1^2}{\varepsilon_2^2} b^0(x, y)^{-1} & \text{if } y \in Y_{\mathbb{P}}^x, \\ 0 & \text{if } y \in Y_{\mathbb{F}}^x. \end{cases} \quad (13)$$

We then define the macroscopic effective permeability by

$$a_{ij}^0(x) = \int_Y \mathbf{e}^i \cdot \mathbf{u}^{j,x} dy \quad \forall i, j \in \{1, \dots, d\}. \quad (14)$$

The meso permeability tensor $b^0 : \Omega \times Y \rightarrow \mathbb{R}^{d \times d}$ depends on the micro porous structure. For any $s = (x, y) \in \Omega \times Y$ we can compute $b^0(s) = b^0(x, y)$ by solving the so-called Stokes micro problems: for any $i \in \{1, \dots, d\}$ find the velocity $\mathbf{u}^{i,s}$ and pressure $p^{i,s}$ such that

$$\begin{aligned} -\Delta \mathbf{u}^{i,s} + \nabla p^{i,s} &= \mathbf{e}^i & \text{in } Z_{\mathbb{F}}^s, & & \mathbf{u}^{i,s} &= 0 & \text{on } \partial Z_{\mathbb{S}}^s, \\ \operatorname{div} \mathbf{u}^{i,s} &= 0 & \text{in } Z_{\mathbb{F}}^s, & & \mathbf{u}^{i,s} \text{ and } p^{i,s} & \text{are } Y\text{-periodic.} \end{aligned} \quad (15)$$

We then define

$$b_{ij}^0(s) = b_{ij}^0(x, y) = \int_{Z_{\mathbb{F}}^s} \mathbf{e}^i \cdot \mathbf{u}^{j,s} dy \quad \forall i, j \in \{1, \dots, d\}. \quad (16)$$

Summary of the presented model problem is shown in Table 1.

Notation. Notice the subtle difference in the notation between the solution of the meso problem (12), denoted by $(\mathbf{u}^{i,x}, p^{i,x})$, and the solution to the micro problem (15), denoted by $(\mathbf{u}^{i,s}, p^{i,s})$. The only difference is that the second index appears in a different space: $x \in \Omega$ and $s \in \Omega \times Y$. In the following sections we will use the same principle to distinguish functions related to either micro or meso scale.

| | macro | meso | micro |
|------------------|----------|------------------------|----------------------------------|
| domain | Ω | $Y = Y_F^x \cup Y_P^x$ | Z_F^s |
| reference domain | | $Y = Y_F \cup Y_P$ | Z_F |
| parameter | | $x \in \Omega$ | $s = (x, y) \in \Omega \times Y$ |
| model problem | (2) | (12), (13), (14) | (15), (16) |

Table 1: A summary of the three-scale model problem in strong form with micro and meso problems in their original domains.

2 Model problem

In this section we provide a weak formulation of the three-scale problem that is summarized in Table 2 and we analyze its well-posedness in section 2.1. The mapping of the micro and meso problems into a reference domain and its well-posedness is described in section 2.2.

2.1. Weak formulation. The macroscopic equation (2) is a standard elliptic problem that can be formulated as follows. Find $p^0 \in H^1(\Omega)/\mathbb{R}$ such that

$$B_0(p^0, q) = L_0(q) \quad \forall q \in H^1(\Omega)/\mathbb{R}, \quad (17)$$

where for any $p, q \in H^1(\Omega)$ we define

$$B_0(p, q) = \int_{\Omega} a^0 \nabla p \cdot \nabla q \, dx, \quad L_0(q) = \int_{\Omega} a^0 \mathbf{f} \cdot \nabla q \, dx.$$

The mesoscopic problem (12) is a typical saddle-point problem. Due to the periodic boundary conditions, pressure is unique only up to an additive constant, which is solved by using a quotient space. For any $x \in \Omega$ and $i \in \{1, \dots, d\}$ we look for $\mathbf{u}^{i,x} \in H_{\text{per}}^1(Y)^d$ and $p^{i,x} \in L^2(Y)/\mathbb{R}$ such that

$$\begin{aligned} \int_Y (\nabla \mathbf{u}^{i,x} : \nabla \mathbf{v} - p^{i,x} \operatorname{div} \mathbf{v} + K^0 \mathbf{u}^{i,x} \cdot \mathbf{v}) \, dy &= \int_Y \mathbf{e}^i \cdot \mathbf{v} \, dy & \forall \mathbf{v} \in H_{\text{per}}^1(Y)^d, \\ - \int_Y q \operatorname{div} \mathbf{u}^{i,x} \, dy &= 0 & \forall q \in L^2(Y)/\mathbb{R}, \end{aligned} \quad (18)$$

where $\nabla \mathbf{u} : \nabla \mathbf{v} = \sum_{i,j=1}^d \partial_i \mathbf{u}_j \partial_i \mathbf{v}_j$ for any vector functions \mathbf{u}, \mathbf{v} , and the space $H_{\text{per}}^1(Y)$ is the set of Y -periodic functions from $H^1(Y)$.

The microscopic problem (15) is a standard Stokes problem. Since there are only Dirichlet and periodic boundary conditions, pressure is again unique only up to an additive constant. The weak formulation reads as follows. For any $s = (x, y) \in \Omega \times Y$ and $i \in \{1, \dots, d\}$ find $\mathbf{u}^{i,s} \in H_{0,\text{per}}^1(Z_F^s)^d$ and $p^{i,s} \in L^2(Z_F^s)/\mathbb{R}$ such that

$$\begin{aligned} \int_{Z_F^s} (\nabla \mathbf{u}^{i,s} : \nabla \mathbf{v} - p^{i,s} \operatorname{div} \mathbf{v}) \, dz &= \int_{Z_F^s} \mathbf{e}^i \cdot \mathbf{v} \, dz & \forall \mathbf{v} \in H_{0,\text{per}}^1(Z_F^s)^d, \\ - \int_{Z_F^s} q \operatorname{div} \mathbf{u}^{i,s} \, dz &= 0 & \forall q \in L^2(Z_F^s)/\mathbb{R}, \end{aligned} \quad (19)$$

where $H_{0,\text{per}}^1(Z_F^s)$ is a subspace of $H^1(Z_F^s)$ that contains Y -periodic functions with a vanishing trace over ∂Z_F^s .

Well-posedness. We will show that the weak formulation of the model problem is well-posed. The microscopic Stokes problem (19) is analogous to the micro problem from the two-scale model. It is shown in [27] that for any $s \in \Omega \times Y$ the problem (19) is well-posed and the effective meso permeability $b^0(s)$ (see (16)) is a symmetric positive definite tensor. Deformations of the micro geometries that guarantee existence of constants $0 < \lambda_b \leq \Lambda_b$ such that

$$b^0(s) \xi \cdot \xi \geq \lambda_b |\xi|^2, \quad |b^0(s) \xi| \leq \Lambda_b |\xi|, \quad \forall \xi \in \mathbb{R}^d, \quad \forall s \in \Omega \times Y \quad (20)$$

have been studied in [1].

Consider next the mesoscopic Stokes–Brinkman problem (18). Symmetry of b^0 implies that K^0 is also symmetric. The estimates (20) guarantee the existence of $0 < \lambda_K \leq \Lambda_K$ such that

$$K^0(x, y)\xi \cdot \xi \geq \lambda_K |\xi|^2, \quad |K^0(x, y)\xi| \leq \Lambda_K |\xi|, \quad \forall \xi \in \mathbb{R}^d, \forall x \in \Omega, \forall y \in Y_F^x. \quad (21)$$

Recall that $K^0(x, y) = 0$ for $y \in Y_F^x$. Assuming sufficient smoothness of φ_{mic} we have for any $x \in \Omega$ that $b^0(x, \cdot) \in L^\infty(Y)^{d \times d}$ and hence $K^0(x, \cdot) \in L^\infty(Y)^{d \times d}$, which makes the meso problem (18) well-defined. The meso problem (18) can be rewritten in a saddle-point formulation as follows. For any $x \in \Omega$ and $i \in \{1, \dots, d\}$ find $\mathbf{u}^{i,x} \in H_{\text{per}}^1(Y)^d$ and $p^{i,x} \in L^2(Y)/\mathbb{R}$ such that

$$\begin{aligned} \tilde{a}(\mathbf{u}^{i,x}, \mathbf{v}; x) + \tilde{b}(\mathbf{v}, p^{i,x}) &= \int_Y \mathbf{e}^i \cdot \mathbf{v} \, dy & \forall \mathbf{v} \in H_{\text{per}}^1(Y), \\ \tilde{b}(\mathbf{u}^{i,x}, q) &= 0 & \forall q \in L^2(Y)/\mathbb{R}, \end{aligned} \quad (22)$$

where $\tilde{a}(\cdot, \cdot; x) : H_{\text{per}}^1(Y)^d \times H_{\text{per}}^1(Y)^d \rightarrow \mathbb{R}$ for any $x \in \Omega$ and $\tilde{b}(\cdot, \cdot) : H_{\text{per}}^1(Y)^d \times L^2(Y)/\mathbb{R} \rightarrow \mathbb{R}$ are bilinear forms defined by

$$\tilde{a}(\mathbf{u}, \mathbf{v}; x) = \int_Y (\nabla \mathbf{u} : \nabla \mathbf{v} + K^0(x, y) \mathbf{u} \cdot \mathbf{v}) \, dy, \quad \tilde{b}(\mathbf{v}, p) = - \int_Y p \operatorname{div} \mathbf{v} \, dy.$$

Since K^0 is symmetric, the bilinear form $\tilde{a}(\cdot, \cdot; x)$ is symmetric too. Let us show that $\tilde{a}(\cdot, \cdot; x)$ is uniformly continuous and bounded. Using (21) we get

$$\tilde{a}(\mathbf{u}, \mathbf{v}; x) \leq \int_Y \nabla \mathbf{u} : \nabla \mathbf{v} + \Lambda_K |\mathbf{u}| |\mathbf{v}| \, dy \leq \Lambda_{\tilde{a}} \|\mathbf{u}\|_{H^1(Y)^d} \|\mathbf{v}\|_{H^1(Y)^d} \quad (23)$$

for every $\mathbf{u}, \mathbf{v} \in H_{\text{per}}^1(Y)^d$ and $x \in \Omega$, where $\Lambda_{\tilde{a}} = \max\{\Lambda_K, 1\}$. For any $\mathbf{u} \in H_{\text{per}}^1(Y)^d$ let $\bar{\mathbf{u}} \in \mathbb{R}^d$ be the average of \mathbf{u} in Y , i.e., $\bar{\mathbf{u}}_i = \int_Y \mathbf{e}^i \cdot \mathbf{u} \, dy$ for every $i \in \{1, \dots, d\}$. Using the lower bound from (21) and the Poincaré–Wirtinger inequality we obtain

$$\begin{aligned} \tilde{a}(\mathbf{u}, \mathbf{u}; x) &\geq \|\nabla \mathbf{u}\|_{L^2(Y)^{d \times d}}^2 + \lambda_K \|\mathbf{u}\|_{L^2(Y_F^x)^d}^2 \\ &\geq C_p \|\mathbf{u} - \bar{\mathbf{u}}\|_{L^2(Y)^d}^2 + \lambda_K \|\mathbf{u}\|_{L^2(Y_F^x)^d}^2 \\ &\geq s \|\mathbf{u}\|_{L^2(Y)^d}^2, \end{aligned} \quad (24)$$

where $s > 0$ depends on C_p, λ_K , and $\inf_{x \in \Omega} |Y_F^x|$. We thus obtain $\tilde{a}(\mathbf{u}, \mathbf{u}; x) \geq s \|\mathbf{u}\|_{L^2(Y)^d}^2$ and using this together with the first line of (24) yields

$$\tilde{a}(\mathbf{u}, \mathbf{u}; x) \geq \lambda_{\tilde{a}} \|\mathbf{u}\|_{H_{\text{per}}^1(Y)^d}^2 \quad \forall \mathbf{u} \in H^1(Y)^d, \quad (25)$$

where $\lambda_{\tilde{a}} = \min\{1, s\}/2$. The bilinear form $\tilde{b}(\cdot, \cdot)$ is inf-sup stable, that is, there exist constants $0 < \lambda_{\tilde{b}} \leq \Lambda_{\tilde{b}}$ such that

$$\begin{aligned} \inf_{\substack{p \in L^2(Y)/\mathbb{R} \\ p \neq 0}} \sup_{\substack{\mathbf{u} \in H_{\text{per}}^1(Y)^d \\ \mathbf{v} \neq 0}} \frac{\tilde{b}(\mathbf{u}, p)}{\|\mathbf{u}\|_{H^1(Y)^d} \|p\|_{L^2(Y)/\mathbb{R}}} &\geq \lambda_{\tilde{b}}, \\ \sup_{\substack{p \in L^2(Y)/\mathbb{R} \\ p \neq 0}} \sup_{\substack{\mathbf{u} \in H_{\text{per}}^1(Y)^d \\ \mathbf{v} \neq 0}} \frac{\tilde{b}(\mathbf{u}, p)}{\|\mathbf{u}\|_{H^1(Y)^d} \|p\|_{L^2(Y)/\mathbb{R}}} &\leq \Lambda_{\tilde{b}}. \end{aligned} \quad (26)$$

The stability conditions (25), (23), and (26) imply that the saddle point problem (22) is well-posed and so is the original meso problem (18). The standard stability estimates give $\|\mathbf{u}^{i,x}\|_{H^1(Y)^d} \leq \lambda_{\tilde{a}}^{-1} \|\mathbf{e}^i\|_{L^2(Y)^d} = \lambda_{\tilde{a}}^{-1}$.

Lemma 4. *Suppose that (23), (25), and (26) hold. Then $a^0(x)$ is symmetric and there exist constants $0 < \lambda_a \leq \Lambda_a$ such that*

$$a^0(x)\xi \cdot \xi \geq \lambda_a |\xi|^2, \quad |a^0(x)\xi| \leq \Lambda_a |\xi|, \quad \forall \xi \in \mathbb{R}^d, \forall x \in \Omega. \quad (27)$$

Proof. The proof is similar to that in [1]. Plugging $\mathbf{v} = \mathbf{u}^{j,x}$ into (22) gives

$$\tilde{a}(\mathbf{u}^{i,x}, \mathbf{u}^{j,x}; x) = \int_Y \mathbf{e}^i \cdot \mathbf{u}^{j,x} \, dy = a_{ij}^0(x). \quad (28)$$

Symmetry of $\tilde{a}(\cdot, \cdot; x)$ then implies symmetry of $a^0(x)$. Using (28) and (23) we obtain

$$\|a^0(x)\|_{\mathbb{F}}^2 = \sum_{i,j=1}^d \tilde{a}(\mathbf{u}^{i,x}, \mathbf{u}^{j,x}; x)^2 \leq \Lambda_{\tilde{a}}^2 \left(\sum_{i=1}^d \|\mathbf{u}^{i,x}\|_{H^1(Y)^d}^2 \right)^2 \leq \frac{d^2 \Lambda_{\tilde{a}}^2}{\lambda_{\tilde{a}}^4} \quad \forall x \in \Omega. \quad (29)$$

For any $\xi \in \mathbb{R}^d$ and $x \in \Omega$ we define $\mathbf{u}^{\xi,x} = \sum_{i=1}^d \xi_i \mathbf{u}^{i,x}$. We then have

$$a^0(x) \xi \cdot \xi = \sum_{i,j=1}^d \tilde{a}(\xi_i \mathbf{u}^{i,x}, \xi_j \mathbf{u}^{j,x}; x) = \tilde{a}(\mathbf{u}^{\xi,x}, \mathbf{u}^{\xi,x}; x) \geq \lambda_{\tilde{a}} \|\mathbf{u}^{\xi,x}\|_{H_{\text{per}}^1(\Omega)^d}^2. \quad (30)$$

Thus, a^0 is at least positive semi-definite for every $x \in \Omega$. Using the Cauchy–Schwarz inequality one can show $\tilde{a}(\mathbf{u}, \mathbf{v}; x)^2 \leq \tilde{a}(\mathbf{u}, \mathbf{u}; x) \tilde{a}(\mathbf{v}, \mathbf{v}; x)$ for any $\mathbf{u}, \mathbf{v} \in H_{\text{per}}^1(Y)^d$. Applying this rule with $\mathbf{u} = \mathbf{u}^{\xi,x}$ in (30) gives

$$a^0(x) \xi \cdot \xi \geq \frac{\tilde{a}(\mathbf{u}^{\xi,x}, \mathbf{v}; x)^2}{\tilde{a}(\mathbf{v}, \mathbf{v}; x)} \quad \forall \mathbf{v} \in H_{\text{per}}^1(Y)^d. \quad (31)$$

If we plug in a constant function $\mathbf{v} \equiv \xi$ we can use the problem (22) and the bound (23) in (31) to obtain

$$a^0(x) \xi \cdot \xi \geq \frac{(\int_Y \xi \cdot \xi \, dy)^2}{\Lambda_{\tilde{a}} \|\xi\|_{H^1(Y)^d}^2} \geq \frac{|\xi|^2}{\Lambda_{\tilde{a}}} \quad \forall \xi \in \mathbb{R}^d. \quad (32)$$

Using (32) and (29) we conclude the proof. \square

Remark 5. Note that in the bound (32) the coercivity constant scales with $\varepsilon_2^2/\varepsilon_1^2$ since Λ_K and therefore $\Lambda_{\tilde{a}}$ scale with $\varepsilon_1^2/\varepsilon_2^2$. In some cases, this can be improved by choosing different test functions \mathbf{v} in (31). Let us recall that the meso geometries $(Y_{\mathbb{F}}^x, Y_{\mathbb{F}}^x)$ are required to satisfy Assumption 2(i) and (ii). If also Assumption 2(iii) holds, then there exist nonzero functions \mathbf{v} in (31) that are supported in $Y_{\mathbb{F}}^x$ and divergence-free. Plugging such function \mathbf{v} into (31) simplifies the bound to

$$a^0(x) \xi \cdot \xi \geq \frac{(\int_{Y_{\mathbb{F}}^x} \xi \cdot \mathbf{v})^2}{|\mathbf{v}|_{H_{0,\text{per}}^1(Y_{\mathbb{F}}^x)^d}^2}.$$

This lower bound was studied in [1] and general criteria on the micro geometries $(Y_{\mathbb{F}}^x, Y_{\mathbb{F}}^x)$ were given to obtain a lower bound on uniform coercivity of a^0 . In this case, this lower bound does not depend on ε_1 and ε_2 .

Finally, we consider the macroscopic problem (17). It is a standard elliptic problem with a positive definite, symmetric, and bounded tensor a^0 . We assume that $a^0 \in L^\infty(\Omega)^{d \times d}$. Notice that such regularity of the homogenized tensor can be proved provided sufficient regularity of the maps φ_{mic} and φ_{mes} . Thus, the macroscopic problem (17) is well-defined and using (27) we can show that

$$\begin{aligned} B_0(p, q) &\leq \Lambda_a |p|_{H^1(\Omega)} |q|_{H^1(\Omega)} & \forall p, q \in H^1(\Omega)/\mathbb{R}, \\ B_0(p, p) &\geq \lambda_a |p|_{H^1(\Omega)}^2 & \forall p \in H^1(\Omega)/\mathbb{R}, \\ L_0(q) &\leq \Lambda_a |q|_{H^1(\Omega)} \|\mathbf{f}\|_{L^2(\Omega)^d} & \forall q \in H^1(\Omega)/\mathbb{R}. \end{aligned}$$

The problem (17) is thus well-posed by the Lax–Milgram lemma and the solution $p^0 \in H^1(\Omega)/\mathbb{R}$ satisfies $|p^0|_{H^1(\Omega)} \leq \Lambda_a / \lambda_a \|\mathbf{f}\|_{L^2(\Omega)^d}$.

2.2. Model problem in reference micro and meso domains. We transform the meso and micro problems in two steps. First, the weak formulation is supplemented with an additional Lagrange multiplier to avoid a quotient space for the pressure variable. Second, a change of variables is used to map the problem to the reference domain. Such modification was already motivated and used in the RB-DS-FE-HMM (see [4]).

Micro problem. After supplementing problem (19) with Lagrange multipliers to fix a zero average of the pressure we map it into the reference micro domain Z_F by applying the change of variables $z_{\text{old}} = \varphi_{\text{mic}}(s, z_{\text{new}})$. Subsequently, we sum the three equations into one, which results in a variational problem in the space $X_{\text{mic}} = H_{0,\text{per}}^1(Z_F) \times L^2(Z_F) \times \mathbb{R}$. We obtain a problem equivalent to (19), (16). For any $s \in \Omega \times Y$ find $\mathbf{U}^{i,s} \in X_{\text{mic}}$ such that

$$A_{\text{mic}}(\mathbf{U}^{i,s}, \mathbf{V}; s) = G_{\text{mic}}^i(\mathbf{V}; s) \quad \forall \mathbf{V} \in X_{\text{mic}}, \quad (33)$$

$$b_{ij}^0(s) = G_{\text{mic}}^i(\mathbf{U}^{j,s}; s) \quad \forall i, j \in \{1, \dots, d\}, \quad (34)$$

where the parameter-dependent bilinear form $A_{\text{mic}}(\cdot, \cdot; s) : X_{\text{mic}} \times X_{\text{mic}} \rightarrow \mathbb{R}$ and linear forms $G_{\text{mic}}^i(\cdot; s) : X_{\text{mic}} \rightarrow \mathbb{R}$ are defined for any $\mathbf{U} = (\mathbf{u}, p, \lambda)$ and $\mathbf{V} = (\mathbf{v}, q, \kappa)$ by

$$A_{\text{mic}}(\mathbf{U}, \mathbf{V}; s) = \int_{Z_F} \sum_{i,j=1}^d \left(\rho_{ij} \frac{\partial \mathbf{u}}{\partial z_i} \cdot \frac{\partial \mathbf{v}}{\partial z_j} - \sigma_{ij} \left(\frac{\partial \mathbf{v}_i}{\partial z_j} p + \frac{\partial \mathbf{u}_i}{\partial z_j} q \right) \right) + \tau(\lambda q + \kappa p) \, dz, \quad (35)$$

$$G_{\text{mic}}^i(\mathbf{V}; s) = \int_{Z_F} \tau \mathbf{e}^i \cdot \mathbf{v} \, dz,$$

where we denote the Jacobian $J = J(s, z) = \nabla_z \varphi_{\text{mic}}(s, z)$ and define

$$\begin{aligned} \rho(s, z) &= \det(J)(J^\top J)^{-1}, \\ \sigma(s, z) &= \det(J)J^{-\top}, \\ \tau(s, z) &= \det(J). \end{aligned} \quad (36)$$

Meso problem. After supplementing problem (18) with Lagrange multipliers we map it into the reference meso structure (Y_F, Y_P) using the change of variables $y_{\text{old}} = \varphi_{\text{mes}}(x, y_{\text{new}})$. Subsequently, we sum the three equations into one, which results in a variational problem in the space $X_{\text{mes}} = H_{\text{per}}^1(Y) \times L^2(Y) \times \mathbb{R}$. We obtain a problem equivalent to (18), (14). For any $x \in \Omega$ and $i \in \{1, \dots, d\}$ find $\mathbf{U}^{i,x} \in X_{\text{mes}}$ such that

$$A_{\text{mes}}(\mathbf{U}^{i,x}, \mathbf{V}; x) = G_{\text{mes}}^i(\mathbf{V}; x) \quad \forall \mathbf{V} \in X_{\text{mes}}, \quad (37)$$

$$b_{ij}^0(x) = G_{\text{mes}}^i(\mathbf{U}^{j,x}; x) \quad \forall i, j \in \{1, \dots, d\}, \quad (38)$$

where the parameter-dependent bilinear form $A_{\text{mes}}(\cdot, \cdot; x) : X_{\text{mes}} \times X_{\text{mes}} \rightarrow \mathbb{R}$ and linear forms $G_{\text{mes}}^i(\cdot; x) : X_{\text{mes}} \rightarrow \mathbb{R}$ are defined for any $\mathbf{U} = (\mathbf{u}, p, \lambda)$ and $\mathbf{V} = (\mathbf{v}, q, \kappa)$ by

$$\begin{aligned} A_{\text{mes}}(\mathbf{U}, \mathbf{V}; x) &= A_{\text{mes}}^{\text{stokes}}(\mathbf{U}, \mathbf{V}; x) + A_{\text{mes}}^{\text{br}}(\mathbf{U}, \mathbf{V}; x), \\ A_{\text{mes}}^{\text{stokes}}(\mathbf{U}, \mathbf{V}; x) &= \int_Y \sum_{i,j=1}^d \left(\rho_{ij} \frac{\partial \mathbf{u}}{\partial y_i} \cdot \frac{\partial \mathbf{v}}{\partial y_j} - \sigma_{ij} \left(\frac{\partial \mathbf{v}_i}{\partial y_j} p + \frac{\partial \mathbf{u}_i}{\partial y_j} q \right) \right) + \tau(\lambda q + \kappa p) \, dy, \\ A_{\text{mes}}^{\text{br}}(\mathbf{U}, \mathbf{V}; x) &= \int_{Y_P} \beta^0 \mathbf{u} \cdot \mathbf{v} \, dy, \end{aligned} \quad (39)$$

$$G_{\text{mes}}^i(\mathbf{V}; x) = \int_Y \tau \mathbf{e}^i \cdot \mathbf{v} \, dy,$$

where we denote the Jacobian $J = J(x, y) = \nabla_y \varphi_{\text{mes}}(x, y)$ and define

$$\begin{aligned} \rho(x, y) &= \det(J)(J^\top J)^{-1}, \\ \sigma(x, y) &= \det(J)J^{-\top}, \\ \tau(x, y) &= \det(J), \\ \beta^0(x, y) &= \frac{\varepsilon_1^2}{\varepsilon_2^2} \det(J)b^0(x, \varphi_{\text{mes}}(x, y))^{-1}. \end{aligned}$$

Well-posedness. Nothing substantial has changed by enforcing the zero pressure average with a Lagrange multiplier and applying the change of variables. The problems (33) and (37) are thus equivalent to (19) and (18), respectively. The regularity assumptions (5) and (6) imply that the standard norms of functions in old and new variables are equivalent. Hence, the problems (37) and (33) are well-posed and there exist constants $0 < \lambda_{\text{mic}} \leq \Lambda_{\text{mic}}$ and $0 < \lambda_{\text{mes}} \leq \Lambda_{\text{mes}}$ such that for every $x \in \Omega$ and $s \in \Omega \times Y$ we have

$$\inf_{\substack{\mathbf{U} \in X_{\text{mic}} \\ \mathbf{U} \neq 0}} \sup_{\substack{\mathbf{V} \in X_{\text{mic}} \\ \mathbf{V} \neq 0}} \frac{A_{\text{mic}}(\mathbf{U}, \mathbf{V}; s)}{\|\mathbf{U}\|_{X_{\text{mic}}} \|\mathbf{V}\|_{X_{\text{mic}}}} \geq \lambda_{\text{mic}}, \quad \sup_{\substack{\mathbf{U} \in X_{\text{mic}} \\ \mathbf{U} \neq 0}} \sup_{\substack{\mathbf{V} \in X_{\text{mic}} \\ \mathbf{V} \neq 0}} \frac{A_{\text{mic}}(\mathbf{U}, \mathbf{V}; s)}{\|\mathbf{U}\|_{X_{\text{mic}}} \|\mathbf{V}\|_{X_{\text{mic}}}} \leq \Lambda_{\text{mic}}, \quad (40)$$

$$\inf_{\substack{\mathbf{U} \in X_{\text{mes}} \\ \mathbf{U} \neq 0}} \sup_{\substack{\mathbf{V} \in X_{\text{mes}} \\ \mathbf{V} \neq 0}} \frac{A_{\text{mes}}(\mathbf{U}, \mathbf{V}; x)}{\|\mathbf{U}\|_{X_{\text{mes}}} \|\mathbf{V}\|_{X_{\text{mes}}}} \geq \lambda_{\text{mes}}, \quad \sup_{\substack{\mathbf{U} \in X_{\text{mes}} \\ \mathbf{U} \neq 0}} \sup_{\substack{\mathbf{V} \in X_{\text{mes}} \\ \mathbf{V} \neq 0}} \frac{A_{\text{mes}}(\mathbf{U}, \mathbf{V}; x)}{\|\mathbf{U}\|_{X_{\text{mes}}} \|\mathbf{V}\|_{X_{\text{mes}}}} \leq \Lambda_{\text{mes}}. \quad (41)$$

Furthermore, there exist constants $L_{\text{mic}}, L_{\text{mes}} \in \mathbb{R}$ such that for every $i \in \{1, \dots, d\}$, $x \in \Omega$ and $s \in \Omega \times Y$ we have

$$\begin{aligned} G_{\text{mic}}^i(\mathbf{V}; s) &\leq L_{\text{mic}} \|\mathbf{V}\|_{X_{\text{mic}}} & \forall \mathbf{V} \in X_{\text{mic}}, \\ G_{\text{mes}}^i(\mathbf{V}; x) &\leq L_{\text{mes}} \|\mathbf{V}\|_{X_{\text{mes}}} & \forall \mathbf{V} \in X_{\text{mes}}. \end{aligned} \quad (42)$$

We note that the tensor β^0 is symmetric, positive definite, and bounded. Hence, the estimates (21) and (6) imply that there exist constants $0 < \lambda_K \leq \Lambda_K$ (the same notation as in (21), for simplicity) such that

$$\beta^0(x, y) \xi \cdot \xi \geq \lambda_K |\xi|^2, \quad |\beta^0(x, y) \xi| \leq \Lambda_K |\xi|, \quad \forall \xi \in \mathbb{R}^d, \quad \forall (x, y) \in \Omega \times Y_{\text{P}}.$$

3 The three-scale numerical method

In this section we propose a new numerical three-scale method for Stokes flow in porous media. It is based on a discretization of the three-scale model problem from section 2.2. The discretization is detailed in section 3.1 and a priori error analysis is provided in section 3.2.

3.1. Finite element discretization. We use a finite element (FE) method to discretize the equations (17), (37), and (33). We proceed in the bottom-up manner, starting with the micro problem. The fully discretized three-scale problem is sketched in Figure 3 and summarized in Table 2.

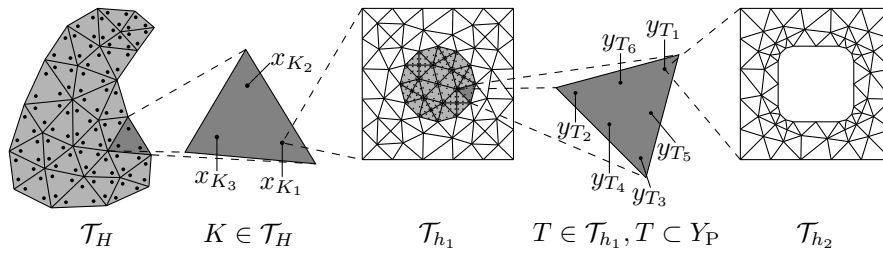


Figure 3: A sketch of the three-scale numerical method. The quadrature formulas correspond to $l = 2$ and $k = 1$.

| | macro | meso | micro |
|--------------------|---------------------------|-----------------------------------|-----------------------------------|
| mesh | \mathcal{T}_H | \mathcal{T}_{h_1} | \mathcal{T}_{h_2} |
| finite elements | \mathcal{P}^l | $\mathcal{P}^{k+1}/\mathcal{P}^k$ | $\mathcal{P}^{m+1}/\mathcal{P}^m$ |
| quadrature formula | (x_{K_j}, ω_{K_j}) | (y_{T_j}, ω_{T_j}) | |
| problem | (49) | (46), (47) | (43), (44) |

Table 2: A summary of the three-scale numerical method.

FE spaces. Let \mathcal{T} be a simplicial mesh of a domain $D \subset \mathbb{R}^d$ and let $n \in \mathbb{N}$. For any element $K \in \mathcal{T}$ we denote by $\mathcal{P}^n(K)$ the space of polynomials in K of degree n . We consider continuous and discontinuous finite element spaces of degree n in \mathcal{T} defined by

$$\begin{aligned} S^n(D, \mathcal{T}) &= \{q \in H^1(D); q|_K \in \mathcal{P}^n(K), \forall K \in \mathcal{T}\}, \\ V^n(D, \mathcal{T}) &= \{q \in L^2(D); q|_K \in \mathcal{P}^n(K), \forall K \in \mathcal{T}\}. \end{aligned}$$

Micro problems. We discretize the micro problem (33) with the Taylor–Hood finite elements $\mathcal{P}^{m+1}/\mathcal{P}^m$ for some $m \in \mathbb{N}$, which is a stable approximation scheme for $m \geq 1$. Let $\{\mathcal{T}_{h_2}\}$ be a family of conformal, shape-regular simplicial meshes of Z_F parametrized by the mesh size $h_2 = \max_{K \in \mathcal{T}_{h_2}} \text{diam}(K)$ and define the FE spaces

$$\begin{aligned} V_{\text{mic}}^{h_2} &= \{\mathbf{v} \in S^{m+1}(Z_F, \mathcal{T}_{h_2})^d; \mathbf{v} \text{ is } Y\text{-periodic}\}, \\ P_{\text{mic}}^{h_2} &= \{q \in S^m(Z_F, \mathcal{T}_{h_2}); q \text{ is } Y\text{-periodic}\}. \end{aligned}$$

Consider $X_{\text{mic}}^{h_2} = V_{\text{mic}}^{h_2} \times P_{\text{mic}}^{h_2} \times \mathbb{R}$, which is a finite-dimensional linear subspace of X_{mic} , and define a numerical approximation of (33) and of the meso permeability (34) as follows. For every $s = (x, y) \in \Omega \times Y$ and $i \in \{1, \dots, d\}$ find $\mathbf{U}_{h_2}^{i,s} \in X_{\text{mic}}^{h_2}$ such that

$$A_{\text{mic}}(\mathbf{U}_{h_2}^{i,s}, \mathbf{V}; s) = G_{\text{mic}}^i(\mathbf{V}; s) \quad \forall \mathbf{V} \in X_{\text{mic}}^{h_2}, \quad (43)$$

$$b_{ij}^{h_2}(s) = G_{\text{mic}}^i(\mathbf{U}_{h_2}^{j,s}; s) \quad \forall i, j \in \{1, \dots, d\}. \quad (44)$$

Meso problems. We discretize the meso problem (37) with the Taylor–Hood finite elements $\mathcal{P}^{k+1}/\mathcal{P}^k$ for some $k \in \mathbb{N}$ with $k \geq 1$. Let $\{\mathcal{T}_{h_1}\}$ be a family of conformal, shape-regular simplicial meshes of Y parametrized by the mesh size $h_1 = \max_{T \in \mathcal{T}_{h_1}} \text{diam}(T)$. We assume that every element $T \in \mathcal{T}_{h_1}$ is either completely in the fluid part ($T \subset Y_F$) or completely in the porous part ($T \subset Y_P$). Let us define the FE spaces

$$\begin{aligned} V_{\text{mes}}^{h_1} &= \{\mathbf{v} \in S^{k+1}(Y, \mathcal{T}_{h_1})^d; \mathbf{v} \text{ is } Y\text{-periodic}\}, \\ P_{\text{mes}}^{h_1} &= \{q \in S^k(Y, \mathcal{T}_{h_1}); q \text{ is } Y\text{-periodic}\}. \end{aligned}$$

Consider a finite dimensional subspace of X_{mes} given by $X_{\text{mes}}^{h_1} = V_{\text{mes}}^{h_1} \times P_{\text{mes}}^{h_1} \times \mathbb{R}$. In the problem (37) we have the term $A_{\text{mes}}^{\text{br}}(\mathbf{U}, \mathbf{V}; x)$ that is related to the mesoscopic permeability. To discretize this term we use numerical quadrature. Let $\mathcal{T}_{h_1}^P \subset \mathcal{T}_{h_1}$ be the subset of all elements contained in Y_P . For each element $T \in \mathcal{T}_{h_1}^P$ we consider a quadrature formula $(y_{T_j}, \omega_{T_j})_{j=1, \dots, J_{\text{mes}}}$ with integration points $y_{T_j} \in K$ and positive weights ω_{T_j} , where $J_{\text{mes}} \in \mathbb{N}$. To achieve the optimal order of accuracy we rely on the following assumption:

$$\int_T q(y) dy = \sum_{j=1}^{J_{\text{mes}}} \omega_{T_j} q(y_{T_j}) \quad \forall T \in \mathcal{T}_{h_1}^P, \quad \forall q \in \mathcal{P}^{2(k+1)}(T), \quad (45)$$

that is, the mesoscopic quadrature formula is exact for polynomials of degree $2(k+1)$. The numerical approximation of (37) and of the macro permeability (38) as follows. For every $x \in \Omega$ and $i \in \{1, \dots, d\}$ find $\mathbf{U}_{h_1}^{i,x} \in X_{\text{mes}}^{h_1}$ such that

$$A_{\text{mes}}^{h_1}(\mathbf{U}_{h_1}^{i,x}, \mathbf{V}; x) = G_{\text{mes}}^i(\mathbf{V}; x) \quad \forall \mathbf{V} \in X_{\text{mes}}^{h_1}, \quad (46)$$

$$a_{ij}^{h_1}(x) = G_{\text{mes}}^i(\mathbf{U}_{h_1}^{j,x}; x) \quad \forall i, j \in \{1, \dots, d\}, \quad (47)$$

where

$$A_{\text{mes}}^{h_1}(\mathbf{U}, \mathbf{V}; x) = A_{\text{mes}}^{\text{stokes}}(\mathbf{U}, \mathbf{V}; x) + \sum_{T \in \mathcal{T}_{h_1}^P} \sum_{j=1}^{J_{\text{mes}}} \omega_{T_j} \beta^{h_2}(x, y_{T_j}) \mathbf{u}(y_{T_j}) \cdot \mathbf{v}(y_{T_j}) dy \quad (48)$$

and $\beta^{h_2} : \Omega \times Y_P \rightarrow \mathbb{R}^{d \times d}$ is defined by

$$\beta^{h_2}(x, y) = \frac{\varepsilon_1^2}{\varepsilon_2^2} \det(\nabla_y \varphi_{\text{mes}}(x, y)) (b^{h_2}(x, \varphi_{\text{mic}}(x, y)))^{-1}.$$

Macro problem. The macroscopic equation (17) is discretized using finite elements of degree $l \in \mathbb{N}$ with numerical quadrature. Macroscopic permeability (47) is upscaled at every macroscopic quadrature point from meso problems. Let $\{\mathcal{T}_H\}$ be a family of conformal, shape-regular simplicial meshes of Ω parametrized by the mesh size $H = \max_{K \in \mathcal{T}_H} \text{diam}(K)$. We consider the macro FE space $S^l(\Omega, \mathcal{T}_H)$ of degree $l \in \mathbb{N}$. For each element $K \in \mathcal{T}_H$ we consider a quadrature formula $(x_{K_j}, \omega_{K_j})_{j=1, \dots, J_{\text{mac}}}$ with integration points $x_{K_j} \in K$ and positive weights ω_{K_j} and $J_{\text{mac}} \in \mathbb{N}$. To guarantee well-posedness of the macroscopic problem and achieve the optimal order of accuracy we suppose that the macroscopic quadrature formulas is exact for polynomials of order $\max(2l - 2, 1)$. A direct discretization of (17) gives: Find $p^H \in S^l(\Omega, \mathcal{T}_H)/\mathbb{R}$ such that

$$B_H(p^H, q^H) = L_H(q^H) \quad \forall q^H \in S^l(\Omega, \mathcal{T}_H)/\mathbb{R}, \quad (49)$$

where the discrete macro bilinear form and right-hand side are given by

$$\begin{aligned} B_H(p^H, q^H) &= \sum_{K \in \mathcal{T}_H} \sum_{j=1}^{J_{\text{mac}}} \omega_{K_j} a^{h_1}(x_{K_j}) \nabla p^H(x_{K_j}) \cdot \nabla q^H(x_{K_j}), \\ L_H(q^H) &= \sum_{K \in \mathcal{T}_H} \sum_{j=1}^{J_{\text{mac}}} \omega_{K_j} a^{h_1}(x_{K_j}) \mathbf{f}^H(x_{K_j}) \cdot \nabla q^H(x_{K_j}). \end{aligned} \quad (50)$$

Here, $\mathbf{f}^H \in V^{l-1}(\Omega, \mathcal{T}_H)^d$ is an appropriate interpolation of the force field $\mathbf{f} \in L^2(\Omega)^d$.

3.2. A priori error estimates. In this section we prove well-posedness of the three-scale numerical method and derive a priori error estimates. Let us start with the micro problem (43). The forms $A_{\text{mic}}(\cdot, \cdot; s)$ and $G_{\text{mic}}(\cdot; s)$ remain continuous with the same constants (see (40) and (42)) also when considered over the FE space $X_{\text{mic}}^{h_2} \subset X_{\text{mic}}$. Taylor–Hood finite elements are stable for approximation of Stokes problems on conforming and shape-regular meshes. Hence, the bilinear form $A_{\text{mic}}(\cdot, \cdot; s)$ remains inf-sup stable also when considered over the FE space $X_{\text{mic}}^{h_2}$. Consequently, there exist constants $0 < \lambda_{\text{mic}} \leq \Lambda_{\text{mic}}$ (denoted the same as in (40), for simplicity of notation) such that

$$\inf_{\substack{\mathbf{U} \in X_{\text{mic}}^{h_2} \\ \mathbf{U} \neq 0}} \sup_{\substack{\mathbf{V} \in X_{\text{mic}}^{h_2} \\ \mathbf{V} \neq 0}} \frac{A_{\text{mic}}(\mathbf{U}, \mathbf{V}; s)}{\|\mathbf{U}\|_{X_{\text{mic}}} \|\mathbf{V}\|_{X_{\text{mic}}}} \geq \lambda_{\text{mic}}, \quad \sup_{\substack{\mathbf{U} \in X_{\text{mic}}^{h_2} \\ \mathbf{U} \neq 0}} \sup_{\substack{\mathbf{V} \in X_{\text{mic}}^{h_2} \\ \mathbf{V} \neq 0}} \frac{A_{\text{mic}}(\mathbf{U}, \mathbf{V}; s)}{\|\mathbf{U}\|_{X_{\text{mic}}} \|\mathbf{V}\|_{X_{\text{mic}}}} \leq \Lambda_{\text{mic}} \quad (51)$$

for every $s \in \Omega \times Y$. The conditions (51), (42), and $X_{\text{mic}}^{h_2} \subset X_{\text{mic}}$ imply that the micro problem (43) is well-posed with a unique solution $\mathbf{U}_{h_2}^{i,s} \in X_{\text{mic}}$ with $\|\mathbf{U}_{h_2}^{i,s}\|_{X_{\text{mic}}} \leq L_{\text{mic}}/\lambda_{\text{mic}}$. Consequently, for any $s \in \Omega \times Y$ and $i, j \in \{1, \dots, d\}$ the permeability $b^{h_2}(s)$ is well-defined in (44) and we can use (44) and (43) to derive

$$b_{ij}^{h_2}(s) = G_{\text{mic}}^i(\mathbf{U}_{h_2}^{j,x}; s) = A_{\text{mic}}(\mathbf{U}_{h_2}^{i,x}, \mathbf{U}_{h_2}^{j,x}; x). \quad (52)$$

Symmetry of A_{mic} and (52) then imply that b^{h_2} is symmetric. For any $\mathbf{V} \in X_{\text{mic}}^{h_2}$ one can derive

$$\begin{aligned} b_{ij}^0(s) - b_{ij}^{h_2}(s) &= G_{\text{mic}}^i(\mathbf{U}^{j,s} - \mathbf{U}_{h_2}^{j,s}; s) \\ &= A_{\text{mic}}(\mathbf{U}^{i,s}, \mathbf{U}^{j,s} - \mathbf{U}_{h_2}^{j,s}; s) \\ &= A_{\text{mic}}(\mathbf{U}^{i,s} - \mathbf{V}, \mathbf{U}^{j,s} - \mathbf{U}_{h_2}^{j,s}; s). \end{aligned} \quad (53)$$

using (44) and (16), then (43) and (33), and finally the Galerkin orthogonality. Using (53) to compute the norm $\|b^0(s) - b^{h_2}(s)\|_{\text{F}}$, applying (40), and taking an infimum over \mathbf{V} gives

$$\|b^0(s) - b^{h_2}(s)\|_{\text{F}}^2 \leq \Lambda_{\text{mic}} \left(\sum_{i=1}^d \inf_{\mathbf{V} \in X_{\text{mic}}^{h_2}} \|\mathbf{U}^{i,s} - \mathbf{V}\|_{X_{\text{mic}}}^2 \right) \left(\sum_{i=1}^d \|\mathbf{U}^{i,s} - \mathbf{U}_{h_2}^{i,s}\|_{X_{\text{mic}}}^2 \right). \quad (54)$$

Lemma 6. Assume that the solution $\mathbf{U}^{i,s} = (\mathbf{u}^{i,s}, p^{i,s}, \lambda^{i,s})$ to the micro problem (33) satisfies $\mathbf{U}^{i,x} \in X_{\text{mic}}^*$, where $X_{\text{mic}}^* = X_{\text{mic}} \cap (H^{m+2}(Z_{\text{F}})^d \times H^{m+1}(Z_{\text{F}}) \times \mathbb{R})$ and that there exists

$C' > 0$ such that $\|\mathbf{U}^{i,s}\|_{X_{\text{mic}}^*} \leq C'$ for every $s \in \Omega \times Y$ and $i \in \{1, \dots, d\}$. Then there is a constant $C > 0$ such that

$$\|b^0(s) - b^{h_2}(s)\|_{\mathbb{F}} \leq Ch_2^{2(m+1)} \quad \forall s \in \Omega \times Y.$$

Proof. For a proof see [14, Lemma 6.3.1]. \square

Even if the micro solutions $\mathbf{U}^{i,s}$ have lower regularity than is assumed in Lemma 6 one still has

$$\lim_{h_2 \rightarrow 0} \inf_{\mathbf{V} \in X_{\text{mic}}^{h_2}} \|\mathbf{U}^{i,s} - \mathbf{V}\|_{X_{\text{mic}}} = 0$$

and therefore

$$\lim_{h_2 \rightarrow 0} \|b^0(s) - b^{h_2}(s)\|_{\mathbb{F}} = 0 \quad \forall s \in \Omega \times Y. \quad (55)$$

Thus, for any $s \in \Omega \times Y$ the permeability $b^{h_2}(s)$ is positive definite for sufficiently small h_2 . If the limit (55) is uniform with respect to $s \in \Omega \times Y$ then for sufficiently small h_2 there are constants $0 < \lambda_b \leq \Lambda_b$ (denoted as in (20) to simplify the notation) such that

$$b^{h_2}(s)\xi \cdot \xi \geq \lambda_b |\xi|^2, \quad |b^{h_2}(s)\xi| \leq \Lambda_b |\xi|, \quad \forall \xi \in \mathbb{R}^d, \quad \forall s \in \Omega \times Y. \quad (56)$$

Even if the limit (55) is not uniform for $s \in \Omega \times Y$, the uniform bounds (56) are valid for sufficiently small $h_2 > 0$ if we restrict the parameter s to $Q^H \times Q^{h_1}$.

We now consider the tensor β^0 and its numerical approximation β^{h_2} . Using (56) and (6) we conclude that β^{h_2} is symmetric and uniformly coercive and bounded. Thus, there are constants $0 < \lambda_K \leq \Lambda_K$ (denoted the same as in (21), for simplicity of notation) such that

$$\beta^{h_2}(x, y)\xi \cdot \xi \geq \lambda_K |\xi|^2, \quad |\beta^{h_2}(x, y)\xi| \leq \Lambda_K |\xi|, \quad \forall \xi \in \mathbb{R}^d, \quad \forall (x, y) \in \Omega \times Y_{\text{P}}. \quad (57)$$

Since b^0 and b^{h_2} are symmetric and with all eigenvalues in the range $[\lambda_b, \Lambda_b]$, there is a constant $C > 0$ such that

$$\|b^0(s)^{-1} - b^{h_2}(s)^{-1}\|_{\mathbb{F}} \leq C \|b^0(s) - b^{h_2}(s)\|_{\mathbb{F}} \quad \forall s \in \Omega \times Y. \quad (58)$$

Let us sketch a proof of the inequality (58). Let M be the set of symmetric matrices with eigenvalues in the interval $[\lambda_b, \Lambda_b]$. It can be shown that M is a connected compact set in $\mathbb{R}^{d \times d}$. Since the mapping $A \rightarrow A^{-1}$ is smooth in M , its derivatives are bounded and the mapping is thus Lipschitz.

Using (58) and (6) we conclude that there is $C > 0$ such that

$$\|\beta^0(s) - \beta^{h_2}(s)\|_{\mathbb{F}} \leq C \|b^0(s) - b^{h_2}(s)\|_{\mathbb{F}} \quad \forall s \in \Omega \times Y_{\text{P}}. \quad (59)$$

We next consider the meso problem (37) and its numerical approximation (46). Since we are using a stable FE pair, the tensor β^{h_2} is coercive and continuous (see (57)), and the quadrature formula satisfies the assumption 45, the problem (46) is well-posed and there are constants $0 < \lambda_{\text{mes}} \leq \Lambda_{\text{mes}}$ (denoted as in (41) to simplify the notation) such that for any $x \in \Omega$ we have

$$\inf_{\substack{\mathbf{U} \in X_{\text{mes}}^{h_1} \\ \mathbf{U} \neq 0}} \sup_{\substack{\mathbf{V} \in X_{\text{mes}}^{h_1} \\ \mathbf{V} \neq 0}} \frac{A_{\text{mes}}^{h_1}(\mathbf{U}, \mathbf{V}; x)}{\|\mathbf{U}\|_{X_{\text{mes}}} \|\mathbf{V}\|_{X_{\text{mes}}}} \geq \lambda_{\text{mes}}, \quad \sup_{\substack{\mathbf{U} \in X_{\text{mes}}^{h_1} \\ \mathbf{U} \neq 0}} \sup_{\substack{\mathbf{V} \in X_{\text{mes}}^{h_1} \\ \mathbf{V} \neq 0}} \frac{A_{\text{mes}}^{h_1}(\mathbf{U}, \mathbf{V}; x)}{\|\mathbf{U}\|_{X_{\text{mes}}} \|\mathbf{V}\|_{X_{\text{mes}}}} \leq \Lambda_{\text{mes}}.$$

Using the same approach as in (52), it can be shown that $a^{h_1}(x)$ is symmetric for any $x \in \Omega$ because of the symmetry of the bilinear form $A_{\text{mes}}^{h_1}$.

Let us now provide a bound for the difference $a^0 - a^{h_1}$. Let $x \in \Omega$ and $i, j \in \{1, \dots, d\}$ be arbitrary. We obtain

$$\begin{aligned} a_{ij}^0(x) - a_{ij}^{h_1}(x) &= G_{\text{mes}}^i(\mathbf{U}^{j,x}; x) - G_{\text{mes}}^i(\mathbf{U}_{h_1}^{j,x}; x) \\ &= A_{\text{mes}}(\mathbf{U}^{i,x}, \mathbf{U}^{j,x}; x) - A_{\text{mes}}^{h_1}(\mathbf{U}_{h_1}^{i,x}, \mathbf{U}_{h_1}^{j,x}; x) \\ &= A_{\text{mes}}(\mathbf{U}^{i,x} - \mathbf{U}_{h_1}^{i,x}, \mathbf{U}^{j,x} - \mathbf{U}_{h_1}^{j,x}; x) \\ &\quad + (A_{\text{mes}} - A_{\text{mes}}^{h_1})(\mathbf{U}_{h_1}^{i,x}, \mathbf{U}_{h_1}^{j,x}; x) \end{aligned} \quad (60)$$

using the definitions (37), (38) and (46), (47). Using the triangle inequality in (60) gives

$$|a_{i_j}^0(x) - a_{i_j}^{h_1}(x)| \leq |E(x)| + |E_1(\mathbf{U}_{h_1}^{i,x}, \mathbf{U}_{h_1}^{j,x}; x)| + |E_2(\mathbf{U}_{h_1}^{i,x}, \mathbf{U}_{h_1}^{j,x}; x)|, \quad (61)$$

where the three functions E , E_1 , and E_2 are defined by

$$\begin{aligned} E(x) &= A_{\text{mes}}(\mathbf{U}^{i,x} - \mathbf{U}_{h_1}^{i,x}, \mathbf{U}^{j,x} - \mathbf{U}_{h_1}^{j,x}; x), \\ E_1(\mathbf{U}, \mathbf{V}; x) &= \int_{Y_{\mathbb{P}}} \beta^0 \mathbf{u} \cdot \mathbf{u} \, dy - \sum_{T \in \mathcal{T}_{h_1}^{\mathbb{P}}} \sum_{j=1}^{J_{\text{mes}}} \omega_{T_j} \beta^0(x, y_{T_j}) \mathbf{u}(y_{T_j}) \cdot \mathbf{v}(y_{T_j}), \\ E_2(\mathbf{U}, \mathbf{V}; x) &= \sum_{T \in \mathcal{T}_{h_1}^{\mathbb{P}}} \sum_{j=1}^{J_{\text{mes}}} \omega_{T_j} (\beta^0(x, y_{T_j}) - \beta^{h_2}(x, y_{T_j})) \mathbf{u}(y_{T_j}) \cdot \mathbf{v}(y_{T_j}), \end{aligned} \quad (62)$$

where $\mathbf{U}, \mathbf{V} \in X_{\text{mes}}^{h_1}$ are arbitrary and $\mathbf{U} = (\mathbf{u}, p, \lambda)$ and $\mathbf{V} = (\mathbf{v}, q, \kappa)$.

Upper bounds for the terms from (62) can be obtained as follows. By (40) we have

$$|E(x)| \leq \Lambda_{\text{mes}} \|\mathbf{U}^{i,x} - \mathbf{U}_{h_1}^{i,x}\|_{X_{\text{mes}}} \|\mathbf{U}^{j,x} - \mathbf{U}_{h_1}^{j,x}\|_{X_{\text{mes}}}. \quad (63)$$

For sufficiently smooth β^0 and non-negative integers $n_1, n_2 \in \mathbb{N}_0$ with $n_1, n_2 \leq k+1$ the error of the quadrature formula can be estimated (see [16, 17]) by

$$|E_1(\mathbf{U}, \mathbf{V}; x)| \leq C h_1^{n_1+n_2} \|\beta^0(x, \cdot)\|_{\bar{W}^{n_1+n_2, \infty}(Y_{\mathbb{P}})^{d \times d}} \|\mathbf{u}\|_{\bar{H}^{n_1}(Y_{\mathbb{P}})^d} \|\mathbf{v}\|_{\bar{H}^{n_2}(Y_{\mathbb{P}})^d}, \quad (64)$$

where $C > 0$ is a constant independent of h_1 . By the norm and triangle inequalities we get

$$|E_2(\mathbf{U}, \mathbf{V}; x)| \leq \max_{y \in Q^{h_1}} \|\beta^0(x, y) - \beta^{h_2}(x, y)\|_{\mathbb{F}} \sum_{T \in \mathcal{T}_{h_1}^{\mathbb{P}}} \sum_{j=1}^{J_{\text{mes}}} \omega_{T_j} |\mathbf{u}(y_{T_j})| |\mathbf{v}(y_{T_j})|. \quad (65)$$

Using the Cauchy–Schwarz inequality and the assumption (45) we obtain

$$\begin{aligned} \sum_{T \in \mathcal{T}_{h_1}^{\mathbb{P}}} \sum_{j=1}^{J_{\text{mes}}} \omega_{T_j} |\mathbf{u}(y_{T_j})| |\mathbf{v}(y_{T_j})| &\leq \left(\sum_{T \in \mathcal{T}_{h_1}^{\mathbb{P}}} \sum_{j=1}^{J_{\text{mes}}} \omega_{T_j} |\mathbf{u}(y_{T_j})|^2 \right)^{\frac{1}{2}} \left(\sum_{T \in \mathcal{T}_{h_1}^{\mathbb{P}}} \sum_{j=1}^{J_{\text{mes}}} \omega_{T_j} |\mathbf{v}(y_{T_j})|^2 \right)^{\frac{1}{2}} \\ &= \|\mathbf{u}\|_{L^2(Y_{\mathbb{P}})^d} \|\mathbf{v}\|_{L^2(Y_{\mathbb{P}})^d} \leq \|\mathbf{U}\|_{X_{\text{mes}}} \|\mathbf{V}\|_{X_{\text{mes}}}. \end{aligned} \quad (66)$$

Combining (65) and (66) gives

$$|E_2(\mathbf{U}, \mathbf{V}; x)| \leq \max_{y \in Q^{h_1}} \|\beta^0(x, y) - \beta^{h_2}(x, y)\|_{\mathbb{F}} \|\mathbf{U}\|_{X_{\text{mes}}} \|\mathbf{V}\|_{X_{\text{mes}}}. \quad (67)$$

Lemma 7. *Assume that the solution $\mathbf{U}^{i,x} = (\mathbf{u}^{i,x}, p^{i,x}, \lambda^{i,x})$ to the meso problem (37) satisfies $\mathbf{U}^{i,x} \in X_{\text{mes}}^*$, where $X_{\text{mes}}^* = X_{\text{mes}} \cap (H^{k+2}(Y)^d \times H^{k+1}(Y) \times \mathbb{R})$ and that $\beta^0(x, \cdot) \in \bar{W}_{\text{per}}^{2(k+1), \infty}(\mathcal{T}_{h_1})^{d \times d}$ for every $x \in \Omega$ and $i \in \{1, \dots, d\}$. Further suppose that there are constants $C', C'' > 0$ such that $\|\mathbf{U}^{i,x}\|_{X_{\text{mes}}^*} \leq C'$ and $\|\beta^0(x, \cdot)\|_{\bar{W}_{\text{per}}^{2(k+1), \infty}(\mathcal{T}_{h_1})^{d \times d}} \leq C''$ for every $x \in \Omega$ and $i \in \{1, \dots, d\}$. Then there is a constant $C > 0$ such that*

$$\|a^0(x) - a^{h_1}(x)\|_{\mathbb{F}} \leq C \left(h_1^{2(k+1)} + \max_{y \in Q^{h_1}} \|\beta^0(x, y) - \beta^{h_2}(x, y)\|_{\mathbb{F}} \right) \quad \forall x \in \Omega. \quad (68)$$

Proof. For a proof see [14, Lemma 6.3.2]. \square

Even if the regularity assumptions of Lemma 7 are not valid the mesoscopic solutions still satisfy

$$\lim_{h_1 \rightarrow 0} \lim_{h_2 \rightarrow 0} \|\mathbf{U}^{i,x} - \mathbf{U}_{h_1}^{i,x}\|_{X_{\text{mes}}} = 0 \quad \forall x \in \Omega,$$

which in turn implies that

$$\lim_{h_1 \rightarrow 0} \lim_{h_2 \rightarrow 0} \|a^0(x) - a^{h_1}(x)\|_{\mathbb{F}} = 0 \quad \forall x \in \Omega. \quad (69)$$

If the limit (69) is uniform with respect to $x \in \Omega$ then for sufficiently small h_1 and h_2 there are constants $0 < \lambda_a \leq \Lambda_a$ (denoted as in (27) to simplify the notation) such that

$$a^{h_1}(x)\xi \cdot \xi \geq \lambda_a |\xi|^2, \quad |a^{h_1}(x)\xi| \leq \Lambda_a |\xi|, \quad \forall \xi \in \mathbb{R}^d, \quad \forall x \in \Omega. \quad (70)$$

Even if the limit (69) is not uniform for $x \in \Omega$, we can have (70) over a finite set $x \in Q^H$.

At the macro scale, the analysis is the same as in the two-scale method. Using the properties (70) and the accuracy of the quadrature formula one can show (see [1, Proposition 3.4]) that

$$\begin{aligned} B_H(q^H, q^H) &\geq \lambda_a |q^H|_{H^1(\Omega)}^2 && \forall q^H \in S^l(\Omega, \mathcal{T}_H), \\ B_H(q^H, r^H) &\leq \Lambda_a |q^H|_{H^1(\Omega)} |r^H|_{H^1(\Omega)} && \forall q^H, r^H \in S^l(\Omega, \mathcal{T}_H), \\ L_H(q^H) &\leq \Lambda_a \|\mathbf{f}^H\|_{L^2(\Omega)^d} |q^H|_{H^1(\Omega)/\mathbb{R}} && \forall q^H \in S^l(\Omega, \mathcal{T}_H). \end{aligned}$$

Thus the macro problem (49) is well-posed and the unique solution can be bounded by $|p^H|_{H^1(\Omega)} \leq \Lambda_a / \lambda_a \|\mathbf{f}^H\|_{L^2(\Omega)^d}$.

Lemma 8. *Suppose that $p^0 \in H^{l+1}(\Omega)$ and that $a^0 \in \bar{W}^{l,\infty}(\Omega)^{d \times d}$. Then there is $C > 0$ such that*

$$|p^0 - p^H|_{H^1(\Omega)} \leq C \left(H^l + \|\mathbf{f} - \mathbf{f}^H\|_{L^2(\Omega)^d} + \|\mathbf{f}^H\|_{L^2(\Omega)^d} \max_{x \in Q^H} \|a^0(x) - a^{h_1}(x)\|_{\mathbb{F}} \right).$$

Proof. The proof follows the a priori error estimates from [1, Section 4]. \square

Theorem 9. *Let the assumptions of Lemma 6, Lemma 7, and Lemma 8 be satisfied and let $\mathbf{f} \in H^l(\Omega)^d$. Then there is a constant $C > 0$ such that*

$$|p^0 - p^H|_{H^1(\Omega)} \leq C(H^l + h_1^{2(k+1)} + h_2^{2(m+1)}).$$

Proof. The result is obtained by using Lemma 8, Lemma 7, estimate (59), and Lemma 6 (in this order). The regularity of \mathbf{f} allows an estimate $\|\mathbf{f} - \mathbf{f}^H\|_{L^2(\Omega)^d} \leq CH^l$ for some $C > 0$. \square

The a priori convergence rate of Theorem 9 is mainly theoretical since the assumed regularity of the micro and meso problems may be difficult to achieve for practical problems. Therefore, non-uniform meshes that are adapted to geometries of macro, meso, or micro domains should be used in practice. Using possibly non-uniform meshes, denoting the number of degrees of freedom by $N_{\text{mac}} = \dim(S^l(\Omega, \mathcal{T}_H))$, $N_{\text{mes}} = \dim(X_{\text{mes}})$, and $N_{\text{mic}} = \dim(X_{\text{mic}})$, the estimate from Theorem 9 reads as

$$|p^0 - p^H|_{H^1(\Omega)} \leq C \left(N_{\text{mac}}^{-\frac{l}{d}} + N_{\text{mes}}^{-\frac{2(k+1)}{d}} + N_{\text{mic}}^{-\frac{2(m+1)}{d}} \right). \quad (71)$$

Since the macroscopic problem is the same as in the two-scale methods from [1, 2, 4], most of the technology that was developed there can be applied in the three-scale problem. For example, it is now straightforward to develop residual-based a posteriori error estimates on the macro scale and provide an adaptive three-scale method or use a conservative macroscopic approximation.

3.3. Computational cost. The computational cost of the three-scale numerical method presented in this section does not depend on the pore sizes ε_1 and ε_2 , they are only present as multiplicative constants in the meso problem (46). We assume that the number of quadrature points we consider on the macro and meso scale is proportional to N_{mac} and N_{mes} , respectively. We thus need to solve one macroscopic problem, $\mathcal{O}(N_{\text{mac}})$ mesoscopic problems, and $\mathcal{O}(N_{\text{mac}}N_{\text{mes}})$ microscopic problems. Further, let us assume that after assembling the computational cost of solving one (micro, meso, or macro) problem is linear in the DOF. The total cost of the three-scale numerical method is then $\mathcal{O}(N_{\text{mac}}N_{\text{mes}}N_{\text{mic}})$. Notice that the micro problems are independent of each other and therefore a parallel implementation of the three-scale method is easily scalable to many threads.

4 Petrov-Galerkin reduced basis method

In the numerical method presented in section 3 the micro and meso problems are solved repeatedly to estimate the effective permeability at meso and macro quadrature points, respectively. In such situations, it is often advantageous to apply a *reduced basis* (RB) method, which can drastically reduce computational costs of the repeated evaluation. In this section we recall the Petrov–Galerkin RB method [3] that has been introduced in [24] and successfully applied in the two-scale settings to the Stokes micro problems in [4]. See [25] for a review of other RB strategies for the Stokes problem.

Non-coercive RB settings. Let X be a Hilbert space with a scalar product $(\cdot, \cdot)_X$ and a corresponding norm $\|\cdot\|_X$ and let \mathcal{D} be a space of parameters. We are interested in a tensor $c(\mu) \in \mathbb{R}^{d \times d}$ for any $\mu \in \mathcal{D}$ that is defined as follows. Find $\mathbf{U}^{i,\mu} \in X$ such that

$$A(\mathbf{U}^{i,\mu}, \mathbf{V}; \mu) = G^i(\mathbf{V}; \mu) \quad \forall \mathbf{V} \in X \quad (72)$$

$$c_{ij}(\mu) = G^i(\mathbf{U}^j; \mu) \quad \forall i, j \in \{1, \dots, d\}, \quad (73)$$

where the parameter-dependent symmetric bilinear form $A(\cdot, \cdot; \mu) : X \times X \rightarrow \mathbb{R}$ and linear forms $G^i(\cdot; \mu) : X \rightarrow \mathbb{R}$ indexed by $i \in \{1, \dots, d\}$ satisfy the following conditions. Assume that there are $0 < \lambda_A \leq \Lambda_A$ and $\Lambda_G \in \mathbb{R}$ such that

$$\inf_{\substack{\mathbf{U} \in X \\ \mathbf{U} \neq 0}} \sup_{\substack{\mathbf{V} \in X \\ \mathbf{V} \neq 0}} \frac{A(\mathbf{U}, \mathbf{V}; \mu)}{\|\mathbf{U}\|_X \|\mathbf{V}\|_X} \geq \lambda_A, \quad \sup_{\substack{\mathbf{U} \in X \\ \mathbf{U} \neq 0}} \sup_{\substack{\mathbf{V} \in X \\ \mathbf{V} \neq 0}} \frac{A(\mathbf{U}, \mathbf{V}; \mu)}{\|\mathbf{U}\|_X \|\mathbf{V}\|_X} \leq \Lambda_A \quad (74)$$

for every $\mu \in \mathcal{D}$ and $G^i(\mathbf{U}) \leq \Lambda_G \|\mathbf{U}\|_X$ for every $\mathbf{U} \in X$ and $i \in \{1, \dots, d\}$. Note that this setting is in agreement with the micro problem (43), (44) and the meso problem (46), (47). Also note that symmetry of A implies that $c(\mu)$ is symmetric.

Petrov-Galerkin projection. For every $i \in \{1, \dots, d\}$ we will construct a linear subspace $X_i \subset X$, where we aim to minimize the projection error of the solutions $\mathbf{U}^{i,x}$ onto X_i for all $x \in \Omega$. For the moment, suppose that X_i is already constructed. We use X_i as a reduced solution space and $X_i^\mu = T(X_i; \mu)$ as a parameter-dependent reduced test space, where $T : X \times \mathcal{D} \rightarrow X$, called the supremizer operator, is defined below. This choice guarantees approximation and algebraic stability of the RB method [3]. The RB approximation of (72) then reads: Find $\mathbf{U}_{\text{RB}}^{i,\mu} \in X_i$ such that

$$A(\mathbf{U}_{\text{RB}}^{i,\mu}, \mathbf{V}; \mu) = G^i(\mathbf{V}; \mu) \quad \forall \mathbf{V} \in X_i^\mu. \quad (75)$$

Supremizer. For any $\mu \in \mathcal{D}$ and $\mathbf{U} \in X$ we choose $T(\mathbf{U}; \mu) \in X$ such that $(T(\mathbf{U}; \mu), \mathbf{V})_X = A(\mathbf{U}, \mathbf{V}; \mu)$ for every $\mathbf{V} \in X$. This variational problem is well-posed and admits a unique solution and the operator $T(\cdot; \mu) : X \rightarrow X$ is linear for any $\mu \in \mathcal{D}$.

Output of interest. While the straightforward approximation the output of interest $c(\mu)$ would be $c_{ij}^{\text{RB}}(\mu) = G^i(\mathbf{U}_{\text{RB}}^{j,\mu}; \mu)$, one can achieve higher accuracy by setting (see [22])

$$c_{ij}^{\text{RB}}(\mu) = G^i(\mathbf{U}_{\text{RB}}^{j,\mu}; \mu) + G^j(\mathbf{U}_{\text{RB}}^{i,\mu}; \mu) - A(\mathbf{U}_{\text{RB}}^{j,\mu}, \mathbf{U}_{\text{RB}}^{i,\mu}; \mu) \quad \forall i, j \in \{1, \dots, d\}. \quad (76)$$

Since A is symmetric, it is evident from (76) that $c^{\text{RB}}(\mu)$ is symmetric too.

Offline/online splitting. The efficiency of the RB method relies on a splitting of the computation into two stages.

- The *offline* stage is run only once and it is used to construct the RB space X_i and precompute necessary values for the online stage.
- The *online* stage can be run after the offline stage repeatedly and it provides a cheap and accurate approximation of the effective permeability $c^{\text{RB}}(\mu)$ for any $\mu \in \mathcal{D}$.

This splitting can be achieved with the following, additional assumption. We assume that there is an affine decomposition of the bilinear form $A(\cdot, \cdot; \mu)$ and of the linear forms $G^i(\cdot; \mu)$, that is, there are $Q_A, Q_G \in \mathbb{N}$ and

- continuous symmetric bilinear forms $A^q(\cdot, \cdot) : X \times X \rightarrow \mathbb{R}$ for $q \in \{1, \dots, Q_A\}$,
- continuous linear forms $G^{iq}(\cdot) : X \rightarrow \mathbb{R}$ for $q \in \{1, \dots, Q_G\}$ and $i \in \{1, \dots, d\}$,
- vector fields $\Theta^A : \mathcal{D} \rightarrow \mathbb{R}^{Q_A}$ and $\Theta^G : \mathcal{D} \rightarrow \mathbb{R}^{Q_G}$,

such that for any $\mathbf{U}, \mathbf{V} \in X$, parameter $\mu \in \mathcal{D}$, and $i \in \{1, \dots, d\}$ we have

$$A(\mathbf{U}, \mathbf{V}; \mu) = \sum_{q=1}^{Q_A} \Theta_q^A(\mu) A^q(\mathbf{U}, \mathbf{V}), \quad G^i(\mathbf{V}; \mu) = \sum_{q=1}^{Q_G} \Theta_q^G(\mu) G^{iq}(\mathbf{V}). \quad (77)$$

RB space. The solution space X_i is spanned by solutions $\mathbf{U}^{i,\mu}$ to (72) for a carefully selected set of parameters $S^i = \{\mu^{i,1}, \mu^{i,2}, \dots, \mu^{i,N_i}\} \subset \mathcal{D}$, where $N_i \in \mathbb{N}$. We consider the sequence $\mathbf{U}^{i,\mu^{i,1}}, \mathbf{U}^{i,\mu^{i,2}}, \dots, \mathbf{U}^{i,\mu^{i,N_i}}$ and apply the Gram–Schmidt orthogonalization procedure to arrive at $\mathbf{U}^{i,1}, \mathbf{U}^{i,2}, \dots, \mathbf{U}^{i,N_i}$. Hence, we have $X_i = \text{span}\{\mathbf{U}^{i,1}, \mathbf{U}^{i,2}, \dots, \mathbf{U}^{i,N_i}\}$. The set S^i is constructed in the offline stage for every $i \in \{1, \dots, d\}$. However, we first consider the online stage.

Online stage. Let us consider the reduced system (75) for any $\mu \in \mathcal{D}$ and $i \in \{1, \dots, d\}$ and let us look for the solution $\mathbf{U}_{\text{RB}}^{i,\mu} \in X_i$ in the form $\mathbf{U}_{\text{RB}}^{i,\mu} = \sum_{n=1}^{N_i} \alpha_n^{i,\mu} \mathbf{U}^{i,n}$, where $\alpha^{i,\mu} = (\alpha_1^{i,\mu}, \dots, \alpha_{N_i}^{i,\mu})^T \in \mathbb{R}^{N_i}$ is a vector of unknowns. We insert this representation into (75) and reduce it into a linear system with unknowns $\alpha^{i,\mu}$. To do that we use the affine decomposition (77) and following decomposition of the supremizer. We have $T(\mathbf{U}; \mu) = \sum_{q=1}^{Q_A} \Theta_q^A(\mu) T^q(\mathbf{U})$, where the linear functionals $T^q : X \rightarrow X$ are defined by variational problems: Find $T^q(\mathbf{U}) \in X$ such that $(T^q(\mathbf{U}), \mathbf{V})_X = A^q(\mathbf{U}, \mathbf{V})$ for every $\mathbf{V} \in X$. Finally, we obtain a reduced system: Find $\alpha^{i,\mu} \in \mathbb{R}^{N_i}$ such that

$$\mathbf{A}^{i,\mu} \alpha^{i,\mu} = \mathbf{G}^{i,\mu}, \quad (78)$$

where the matrix $\mathbf{A}^{i,\mu} \in \mathbb{R}^{N_i \times N_i}$ and the vector $\mathbf{G}^{i,\mu} \in \mathbb{R}^{N_i}$ are defined entry-wise by

$$\begin{aligned} (\mathbf{A}^{i,\mu})_{nm} &= \sum_{q,r=1}^{Q_A} \Theta_q^A(\mu) \Theta_r^A(\mu) \underline{A^q(\mathbf{U}^{i,n}, T^r(\mathbf{U}^{i,m}))}, & \forall n, m \in \{1, \dots, N_i\}, \\ (\mathbf{G}^{i,\mu})_n &= \sum_{q=1}^{Q_A} \sum_{r=1}^{Q_G} \Theta_q^A(\mu) \Theta_r^G(\mu) \underline{G^{ir}(T^q(\mathbf{U}^{i,n}))}, & \forall n \in \{1, \dots, N_i\}. \end{aligned} \quad (79)$$

As the underlined quantities in (79) can be precomputed in the offline stage, the assembling of (79) and the solution of (78) have a time cost independent of $\dim(X)$. Indeed, the assembling of (79) takes $\mathcal{O}(N_i^2 Q_A^2 + N_i Q_A Q_G)$ operations. The linear system (78) is dense but of small size N_i , therefore, a direct solution takes $\mathcal{O}(N_i^3)$ operations. Applying the affine decomposition in the definition of $c^{\text{RB}}(x)$ in (76) gives

$$\begin{aligned} c_{ij}^{\text{RB}}(\mu) &= \sum_{q=1}^{Q_G} \Theta_q^G(\mu) \left(\sum_{m=1}^{N_j} \alpha_m^{j,\mu} \underline{G^{iq}(\mathbf{U}^{j,m})} + \sum_{n=1}^{N_i} \alpha_n^{i,\mu} \underline{G^{jq}(\mathbf{U}^{i,n})} \right) \\ &\quad - \sum_{q=1}^{Q_A} \sum_{n=1}^{N_i} \sum_{m=1}^{N_j} \alpha_n^{i,\mu} \alpha_m^{j,\mu} \Theta_q^A(\mu) \underline{A^q(\mathbf{U}^{i,n}, \mathbf{U}^{j,m})}. \end{aligned} \quad (80)$$

Again, by precomputing the underlined expressions in the offline stage, the evaluation of $c^{\text{RB}}(\mu)$ is independent of $\dim(X)$.

A posteriori error estimate. The offline stage relies on a cheap and accurate error estimator. Given a RB space X_i , we can show that

$$\|\mathbf{U}^{i,\mu} - \mathbf{U}_{\text{RB}}^{i,\mu}\|_X \leq \Delta_i^{\text{E}}(\mu) := \frac{\|R^i(\cdot; \mu)\|_{X'}}{\beta_{\text{LB}}(\mu)}, \quad (81)$$

where $R^i(\mathbf{V}; \mu) = G^i(\mathbf{V}; \mu) - A(\mathbf{U}_{\text{RB}}^{i,\mu}, \mathbf{V}; \mu)$ and $\beta_{\text{LB}}(\mu)$ is a positive lower bound of the inf-sup stability constant $\beta(\mu)$ of $A(\cdot, \cdot; \mu)$. We outline some ways to cheaply compute $\beta_{\text{LB}}(\mu)$ below. The residual term $\|R^i(\cdot; \mu)\|_{X'}$ can be evaluated using

$$\|R^i(\cdot; \mu)\|_{X'}^2 = \sum_{q,r=1}^{Q_G} \Theta_q^G(\mu) \Theta_r^G(\mu) \underline{(\mathbf{P}^{iq}, \mathbf{P}^{ir})_X} - 2\mathbf{G}^{i,\mu} \cdot \alpha^{i,\mu} + \mathbf{A}^{i,\mu} \alpha^{i,\mu} \cdot \alpha^{i,\mu}, \quad (82)$$

where \mathbf{P}^{iq} the unique element of X such that $(\mathbf{P}^{iq}, \mathbf{V})_X = G^{iq}(\mathbf{V})$ for every $\mathbf{V} \in X$. The underlined terms can be computed in the offline stage, which makes the time cost of evaluating $\|R^i(\cdot; \mu)\|_{X'}$ independent of $\dim(X)$.

In the following algorithm we outline how the parameters $S^i = \{\mu^{i,1}, \dots, \mu^{i,N_i}\}$, which define the RB space X_i , are selected using a greedy procedure. For details see [3, 4].

Algorithm 10 (greedy RB construction). We select a training set of parameters $\Xi_{\text{train}} \subset \mathcal{D}$ and a tolerance $\varepsilon_{\text{RB}} > 0$. For each $i \in \{1, \dots, d\}$ we start with $S^i = \emptyset$ and repeat:

1. Find $\bar{\mu} \in \Xi_{\text{train}}$ for which the value $\Delta_i^{\text{E}}(\bar{\mu})$ is the largest.
2. If $\Delta_i^{\text{E}}(\bar{\mu}) < \varepsilon_{\text{RB}}$, we stop the algorithm. Else, we add $\bar{\mu}$ to S^i and update the space X_i .

Inf-sup lower bound $\beta_{\text{LB}}(\mu)$. The a posteriori error estimate (81) contains an inf-sup lower bound $0 < \beta_{\text{LB}}(\mu) \leq \beta(\mu)$ that we need to evaluate for every $\mu \in \Xi_{\text{train}}$. For any $\mu \in \mathcal{D}$ the inf-sup constant $\beta(\mu)$ can be interpreted as $\sqrt{\lambda_{\min}}$, where λ_{\min} is a minimal eigenvalue of a generalized eigenvalue problem of the type $Az = \lambda Bz$ with A and B symmetric and positive definite. However, solving this eigenproblem numerically for every $\mu \in \Xi_{\text{train}}$ can be prohibitive. The successive constraint method [20] is a greedy offline-online algorithm that computes $\beta(\bar{\mu})$ exactly for a small number of parameters $\bar{\mu} \in S \subset \Omega$ and then uses a rigorous bound $\beta(\mu) \geq \beta_{\text{SCM}}(\mu) := \max_{\bar{\mu} \in S} \beta(\bar{\mu}) \beta_{\text{LB}}(\mu; \bar{\mu})$, where the online computation of the term $\beta_{\text{LB}}(\mu; \bar{\mu})$ involves solving a small linear programming problem. We can thus perform the SCM offline stage before the RB offline stage and then use β_{SCM} in the estimate (82).

While SCM is an improvement to computing $\beta(\mu)$ exactly, it can still be the main bottleneck of the offline and also online stage [4]. In practice, one achieves good approximation properties of the space X_i also if we have only $\beta_{\text{LB}}(\mu) \approx C\beta(\mu)$. Some cheaper methods to define $\beta_{\text{LB}}(\mu)$ based on a simple interpolation are discussed in [4].

A priori error estimates. It can be shown (see [4]) that there is $C > 0$ depending only on λ_A and Λ_A such that

$$\|c(\mu) - c^{\text{RB}}(\mu)\|_{\text{F}} \leq C \sum_{i=1}^d \inf_{\mathbf{V} \in X_i} \|\mathbf{U}^{i,x} - \mathbf{V}\|_X^2. \quad (83)$$

A priori theory for approximability of the solution manifold $\mathcal{M}^i = \{\mathbf{U}^{i,\mu}; \mu \in \mathcal{D}\} \subset X$ by the RB space X_i relies on the notion of Kolmogorov n -width, which is defined by

$$d_n(\mathcal{M}^i) = \inf_{\substack{Z \subset X \\ \dim(Z)=n}} \sup_{\mathbf{U} \in \mathcal{M}^i} \inf_{\mathbf{V} \in Z} \|\mathbf{U} - \mathbf{V}\|_X. \quad (84)$$

In [11] it is proved for coercive problems that if $d_n(\mathcal{M}^i)$ is decreasing exponentially ($d_n(\mathcal{M}^i) \leq ae^{-bn^c}$) or following a power law ($d_n(\mathcal{M}^i) \leq an^{-b}$), then so is $\inf_{\mathbf{V} \in X_i} \|\mathbf{U}^{i,x} - \mathbf{V}\|_X$, with some different the constants a, b, c . While Stokes problem is not coercive, our RB formulation (75) can be equivalently rewritten as follows: Find $\mathbf{U}_{\text{RB}}^{i,x} \in X_i$ such that

$$B(\mathbf{U}_{\text{RB}}^{i,x}, \mathbf{V}; x) = G^i(\mathbf{V}; x) \quad \forall \mathbf{V} \in X_i,$$

where the parameter-dependent bilinear form

$$B(\mathbf{U}, \mathbf{V}; x) = (T(\mathbf{U}; x), T(\mathbf{V}; x))_X \quad \forall \mathbf{U}, \mathbf{V} \in X$$

is symmetric and positive definite. It can be shown (see [4] for details) that the a posteriori error estimator is uniformly equivalent to the exact error

$$\inf_{\mathbf{V} \in X_i} \|\mathbf{U}^{i,\mu} - \mathbf{V}\|_X \leq \Delta_i^{\text{E}}(\mu) \leq \frac{\Lambda_A}{\lambda_A} \left(1 + \frac{\Lambda_A}{\lambda_A}\right) \inf_{\mathbf{V} \in X_i} \|\mathbf{U}^{i,\mu} - \mathbf{V}\|_X$$

and hence the a priori error estimates for coercive problems [11] are applicable. In terms of the tolerance that we prescribe to the offline greedy algorithm, one can show that there is a constant $C > 0$ such that

$$\|c(\mu) - c^{\text{RB}}(\mu)\|_{\text{F}} \leq C\varepsilon_{\text{RB}}^2 \quad (85)$$

that is valid for every training parameter $\mu \in \Xi_{\text{train}}$. However, if the training set is dense enough in \mathcal{D} it is reasonable to assume that (85) is true for any $\mu \in \mathcal{D}$ with some $C > 0$.

5 Reduced basis three-scale numerical method

In this section we propose a new reduced basis three-scale numerical method for Stokes flow in porous media. We depart from the three-scale numerical method described in section 3 and apply the RB method from section 4 to the meso and micro scale. We build this new method bottom-up, starting with the micro scale. Application of the RB method at the micro scale is similar as in the two-scale problem (see [4]). However, there is no direct way to obtain an affine decomposition of the meso problem, which is a fundamental assumption for an efficient RB method. We solve this obstacle by an approximate expansion of the mesoscopic bilinear form obtained by the empirical interpolation method [8].

Affine decomposition of the micro problem. The micro problem (43), (44) has the same form as (72), (73). Micro problems are parametrized by $s \in \Omega \times Y_{\text{P}}$, which corresponds to $\mu = s$ and $\mathcal{D} = \Omega \times Y_{\text{P}}$, and we work in the Hilbert space $X = X_{\text{mic}}^{h_2}$. To apply the RB method we need to provide an affine decomposition of the type (77) for A_{mic} and G_{mic}^i . Let us start with the affine forms G_{mic}^i . Using (36) in (35) gives $G_{\text{mic}}^i(\mathbf{V}; s) = \int_{Z_{\text{F}}} \det(\nabla_z \varphi_{\text{mic}}(s, z)) \mathbf{e}^i \cdot \mathbf{v} \, dz$ for every $\mathbf{V} = (\mathbf{v}, q, \kappa) \in X_{\text{mic}}^{h_2}$. Our goal is to write $G_{\text{mic}}^i(\mathbf{V}; s)$ as a sum of products of functions depending only on s and only on \mathbf{V} . A standard way to provide such decomposition is with the following assumption on the geometry transformation φ_{mic} .

Assumption 11. Let $R_{\text{mic}} \in \mathbb{N}$ and assume that $\{Z_{\text{F}}^r\}_{r=1}^{R_{\text{mic}}}$ is a disjoint partition of Z_{F} such that the restriction $\varphi_{\text{mic}}(s, z)|_{z \in Z_{\text{F}}^r}$ is affine for every $s \in \Omega \times Y$ and $r \in \{1, \dots, R_{\text{mic}}\}$. Moreover, for any $K \in \mathcal{T}_{h_2}$ there is $r \in \{1, \dots, R_{\text{mic}}\}$ such that $K \in Z_{\text{F}}^r$.

Assumption 11 implies that $\nabla_z \varphi_{\text{mic}}(s, z)$ is constant in $z \in Z_{\text{F}}^r$ for every $s \in \Omega \times Y$. Using this in the definition (36) we obtain that for any $s \in \Omega \times Z_{\text{F}}^r$ we have

$$\begin{aligned} \rho(s, z) &= \rho^r(s) := \det(J^r(s))(J^r(s))^{\top} J^r(s)^{-1}, \\ \sigma(s, z) &= \sigma^r(s) := \det(J^r(s)) J^r(s)^{-\top}, \\ \tau(s, z) &= \tau^r(s) := \det(J^r(s)), \end{aligned}$$

where the Jacobian $J^r(s)$ is the constant value of $\nabla_z \varphi_{\text{mic}}(s, z)$ for $z \in Z_{\text{F}}^r$. Hence, the bilinear form A_{mic} and the linear forms G_{mic}^i can be affinely decomposed as follows. For any $\mathbf{U} = (\mathbf{u}, p, \lambda) \in X$, $\mathbf{V} = (\mathbf{v}, q, \kappa) \in X$, and $s \in \Omega \times Y$ we have

$$\begin{aligned} A_{\text{mic}}(\mathbf{U}, \mathbf{V}; s) &= \sum_{i,j=1}^d \sum_{r=1}^{R_{\text{mic}}} \rho_{ij}^r(s) \int_{Z_{\text{F}}^r} \frac{\partial \mathbf{u}}{\partial z_i} \cdot \frac{\partial \mathbf{v}}{\partial z_j} \, dz \\ &\quad - \sum_{i,j=1}^d \sum_{r=1}^{R_{\text{mic}}} \sigma_{ij}^r(s) \int_{Z_{\text{F}}^r} \left(\frac{\partial \mathbf{v}_i}{\partial z_j} p + \frac{\partial \mathbf{u}_i}{\partial z_j} q \right) \, dz \\ &\quad + \sum_{r=1}^{R_{\text{mic}}} \tau^r(s) \int_{Z_{\text{F}}^r} (\lambda q + \kappa p) \, dz, \\ G_{\text{mic}}^i(\mathbf{V}; s) &= \sum_{r=1}^{R_{\text{mic}}} \tau^r(s) \int_{Z_{\text{F}}^r} \mathbf{e}^i \cdot \mathbf{v} \, dz. \end{aligned} \quad (86)$$

Using symmetry of ρ and σ we can obtain an affine decomposition of A_{mic} with $Q_A^{\text{mic}} = R_{\text{mic}}(1 + d + d^2)$. The affine decomposition of G^i has $Q_G^{\text{mic}} = R_{\text{mic}}$ terms.

RB at the micro scale. Thus, all the requirements of the RB method are met. We set the tolerance $\varepsilon_{\text{mic}}^{\text{RB}} > 0$ and choose a training set of parameters $\Xi_{\text{mic}}^{\text{RB}} \subset \Omega \times Y_{\text{P}}$ and the RB offline computation can start by running Algorithm 10. The RB approximation of the solution $\mathbf{U}_{h_2}^{i,s}$ is denoted by $\mathbf{U}_{\text{RB}}^{i,s}$ and the resulting approximation of $b^{h_2}(s)$ by the RB method (see (76)) is defined by

$$b_{ij}^{\text{RB}}(s) = G_{\text{mic}}^i(\mathbf{U}_{\text{RB}}^{j,s}; s) + G_{\text{mic}}^j(\mathbf{U}_{\text{RB}}^{i,s}; s) - A_{\text{mic}}(\mathbf{U}_{\text{RB}}^{i,s}, \mathbf{U}_{\text{RB}}^{j,s}; s).$$

Affine decomposition of the meso problem. We update the meso problem (46), (47) to include the upscaled meso permeability b^{RB} instead of b^{h_2} . We replace the bilinear form $A_{\text{mes}}^{h_1}$ (defined in (48)) with

$$A_{\text{mes}}^{\text{RB}}(\mathbf{U}, \mathbf{V}; x) = A_{\text{mes}}^{\text{stokes}}(\mathbf{U}, \mathbf{V}; x) + \sum_{T \in \mathcal{T}_{h_1}^{\text{P}}} \sum_{j=1}^{J_{\text{mes}}} \omega_{T_j} \beta^{\text{RB}}(x, y_{T_j}) \mathbf{u}(y_{T_j}) \cdot \mathbf{v}(y_{T_j}) \, dy, \quad (87)$$

where $\beta^{\text{RB}} : \Omega \times Y_{\text{P}} \rightarrow \mathbb{R}^{d \times d}$ is defined by

$$\beta^{\text{RB}}(x, y) = \frac{\varepsilon_1^2}{\varepsilon_2^2} \det(\nabla_y \varphi_{\text{mes}}(x, y)) (b^{\text{RB}}(x, \varphi_{\text{mic}}(x, y)))^{-1}.$$

From now on we consider the meso problem with the bilinear form (87) and the original right-hand side G^i as in (46). Meso problems have the same structure as the model problem in section 4. They are parametrized by $x \in \Omega$, which corresponds to $\mu = x$ and $\mathcal{D} = \Omega$, and we use the Hilbert space $X = X_{\text{mes}}^{h_1}$. To successfully apply the RB method we need to provide an affine decomposition (77) to the bilinear form $A_{\text{mes}}^{\text{RB}}$ and to the linear forms G_{mes}^i defined in (39). Let us start with an additional assumption on φ_{mes} that will help us with a part of the decomposition.

Assumption 12. Let $R_{\text{mes}} \in \mathbb{N}$ and assume that $\{Y^r\}_{r=1}^{R_{\text{mes}}}$ is a disjoint partition of Y such that the restriction $\varphi_{\text{mes}}(x, y)|_{y \in Y^r}$ is linear for every $x \in \Omega$ and $r \in \{1, \dots, R_{\text{mes}}\}$. Moreover, for every $T \in \mathcal{T}_{h_1}$ there is $r \in \{1, \dots, R_{\text{mes}}\}$ such that $T \in Y^r$.

Using Assumption 12 we can repeat the reasoning we used with the micro problems to show that the linear forms G_{mes}^i and the bilinear form $A_{\text{mes}}^{\text{stokes}}$ allow an affine decomposition with Q_G^{mes} and Q_A^{mes} terms, respectively. However, we cannot apply the same reasoning to the term with quadrature formula in (87) since a form of the function $\beta^{\text{RB}}(x, y)$ that would separate x and y is not known. This problem can be solved by considering a suitable approximation of (87) given by the empirical interpolation method described below. For the moment, let us assume that we have an approximate expansion

$$\beta^{\text{EIM}}(x, y) = \sum_{n=1}^{N_{\text{EIM}}} q^n(y) r^n(x) \approx \beta^{\text{RB}}(x, y), \quad (88)$$

where $q^n : Y_{\text{P}} \rightarrow \mathbb{R}^{d \times d}$ and $r^n : \Omega \rightarrow \mathbb{R}$ for $n \in \{1, \dots, N_{\text{EIM}}\}$ and $N_{\text{EIM}} \in \mathbb{N}$. We then substitute the expansion (88) in (87) and define

$$A_{\text{mes}}^{\text{EIM}}(\mathbf{U}, \mathbf{V}; x) = A_{\text{mes}}^{\text{stokes}}(\mathbf{U}, \mathbf{V}; x) + \sum_{T \in \mathcal{T}_{h_1}^{\text{P}}} \sum_{j=1}^{J_{\text{mes}}} \omega_{T_j} \beta^{\text{EIM}}(x, y_{T_j}) \mathbf{u}(y_{T_j}) \cdot \mathbf{v}(y_{T_j}) \, dy. \quad (89)$$

Let the affine decomposition of $A_{\text{mes}}^{\text{stokes}}(\mathbf{U}, \mathbf{V}; x)$ be composed of coefficients $\Theta_q^A(x)$ and non-parametric bilinear forms $A^q(\mathbf{U}, \mathbf{V})$, where the index q is in range $\{N_{\text{EIM}} + 1, \dots, N_{\text{EIM}} + Q_A^{\text{mes}}\}$. Changing the summation order in (89) and applying (88) and the affine decomposition of $A_{\text{mes}}^{\text{stokes}}$ gives

$$\begin{aligned} A_{\text{mes}}^{\text{EIM}}(\mathbf{U}, \mathbf{V}; x) &= \sum_{n=1}^{N_{\text{EIM}}} \underbrace{r^n(x)}_{=: \Theta_n^A(x)} \underbrace{\sum_{T \in \mathcal{T}_{h_1}^{\text{P}}} \sum_{j=1}^{J_{\text{mes}}} \omega_{T_j} q^n(y_{T_j}) \mathbf{u}(y_{T_j}) \cdot \mathbf{v}(y_{T_j}) \, dy}_{=: A^n(\mathbf{U}, \mathbf{V})} \\ &+ \sum_{q=N_{\text{EIM}}+1}^{N_{\text{EIM}}+Q_A^{\text{mes}}} \Theta_q^A(x) A^q(\mathbf{U}, \mathbf{V}). \end{aligned}$$

Updated meso problem. At the meso scale we replace the original problem (46), (47) with the following approximation. For every $x \in \Omega$ and $i \in \{1, \dots, d\}$ find $\mathbf{U}_{\text{EIM}}^{i,x} \in X_{\text{mes}}^{h_1}$ such that

$$A_{\text{mes}}^{\text{EIM}}(\mathbf{U}_{\text{EIM}}^{i,x}, \mathbf{V}; x) = G_{\text{mes}}^i(\mathbf{V}; x) \quad \forall \mathbf{V} \in X_{\text{mes}}^{h_1}, \quad (90)$$

$$a_{ij}^{\text{EIM}}(x) = G_{\text{mes}}^i(\mathbf{U}_{h_1}^{j,x}; x) \quad \forall i, j \in \{1, \dots, d\}. \quad (91)$$

We have shown that Assumption 12 and the approximate expansion (88) imply that $A_{\text{mes}}^{\text{EIM}}$ and G_{mes}^i have affine decompositions of sizes $Q_A^{\text{mes}} + N_{\text{EIM}}$ and Q_G^{mes} , respectively. Let us explain the last piece of the meso RB method, the construction of (88).

Empirical interpolation method. An approximate expansion such as (88) can be constructed using the empirical interpolation method [8]. For brevity we explain the method in a general setting and then show how it applies to our problem.

Consider sets \mathcal{D} and \mathcal{P} and a function $f : \mathcal{D} \times \mathcal{P} \rightarrow \mathbb{R}$. We build a sequence of approximations of f denoted by $I_N[f] : \mathcal{D} \times \mathcal{P} \rightarrow \mathbb{R}$ indexed by $N \in \{0, 1, \dots, N_{\text{EIM}}\}$, where $N_{\text{EIM}} \in \mathbb{N}$ is the final size of the approximation. With an offline greedy algorithm (see below) we construct the so-called magic points $y_n \in \mathcal{P}$ and functions $q^n : \mathcal{P} \rightarrow \mathbb{R}$ for $n \in \{1, \dots, N_{\text{EIM}}\}$. We then define $I_0[f](x, y) \equiv 0$ and for $N \geq 1$ we let

$$I_N[f](x, y) = \sum_{n=1}^N q^n(y) \left(\sum_{m=1}^N B_{nm}^N f(x, y_m) \right), \quad (92)$$

where B^N is the inverse of the matrix $(q_m(y_n))_{1 \leq n, m \leq N}$. The coefficients that multiply q^n in (92) can be computed in the online stage with only N evaluations of the function f and one matrix-vector multiplication with the matrix of size $N \times N$. Let us define the error of the EIM approximation simply by

$$E_N[f](x, y) = f(x, y) - I_N[f](x, y).$$

Algorithm 13 (EIM offline stage). Set a tolerance $\varepsilon_{\text{EIM}} > 0$. For $n = 0, 1, \dots$ do:

1. Find where the interpolation commits the largest pointwise error:

$$x_{n+1}, y_{n+1} \leftarrow \arg \max_{x \in \mathcal{D}, y \in \mathcal{P}} |E_n[f](x, y)|. \quad (93)$$

If $|E_n[f](x_{n+1}, y_{n+1})| < \varepsilon_{\text{EIM}}$ then we stop iterating and let $N_{\text{EIM}} \leftarrow n$.

2. We define $q^{n+1} : \mathcal{P} \rightarrow \mathbb{R}$ as

$$q^{n+1}(y) \leftarrow \frac{E_n[f](x_{n+1}, y)}{E_n[f](x_{n+1}, y_{n+1})}.$$

Application of EIM to obtain (88). For several reasons it is not straightforward to apply the EIM to obtain the expansion (88). First, values of the function $\beta^{\text{RB}}(x, y)$ are not real numbers but real matrices of size $d \times d$. Second, the set $\Omega \times Y_{\text{P}}$ is infinite, therefore, a direct evaluation of expressions as (93) can be problematic. We address the first point by considering a function $f : \Omega \times (Y_{\text{P}} \times \{1, \dots, d\}^2) \rightarrow \mathbb{R}$ defined by

$$f(x, (y, i, j)) = \beta_{ij}^{\text{RB}}(x, y).$$

The second point can be addressed by taking only finite samples of Ω and Y_{P} that we denote by $\mathcal{D} = \Xi_{\text{mes}}^{\text{EIM}} \subset \Omega$ and $\mathcal{P} = \Xi_{\text{mes}}^{\text{EIM}} \subset Y_{\text{P}}$, respectively. The offline EIM algorithm then becomes numerically feasible. We obtain $N_{\text{EIM}} \in \mathbb{N}$ and a sequence of magic points $(y_n, i_n, j_n) \in Y_{\text{P}} \times \{1, \dots, d\}^2$ and functions $q^n : Y_{\text{P}} \times \{1, \dots, d\}^2 \rightarrow \mathbb{R}$ for $n \in \{1, \dots, N_{\text{EIM}}\}$. The real functions q^n are then reshaped into matrix-valued functions by $q_{ij}^n(y) = q^n(y, i, j)$. Thus, we define

$$\beta^{\text{EIM}}(x, y) = \sum_{n=1}^{N_{\text{EIM}}} q^n(y) \underbrace{\left(\sum_{m=1}^{N_{\text{EIM}}} B_{nm} \beta_{i_m j_m}^{\text{RB}}(x, y_m) \right)}_{=: r^n(x)}, \quad (94)$$

which is a decomposition of the desired form (88). Given a tolerance ε_{EIM} , we can perform the offline EIM algorithm and it is guaranteed that

$$\|\beta^{\text{RB}}(x, y) - \beta^{\text{EIM}}(x, y)\|_{\text{F}} \leq C\varepsilon_{\text{EIM}} \quad (95)$$

for every $(x, y) \in \Xi_{\text{mac}}^{\text{EIM}} \times \Xi_{\text{mes}}^{\text{EIM}}$. If the training samples are dense enough in $\Omega \times Y_{\text{P}}$ we expect that the inequality (95) holds for every $(x, y) \in Q^H \times Q^{h_1}$. We advise to choose $\Xi_{\text{mac}}^{\text{EIM}} \subset Q^H$ (quadrature points of the initial macro mesh) and $\Xi_{\text{mes}}^{\text{EIM}} \subset Q^{h_1}$ (quadrature points of the mesoscopic mesh used to compute the RB functions) so that the training sets contain only a fraction of the total number of the quadrature points.

RB at the meso scale. An affine decomposition of the modified meso problem (90) has been provided and thus the requirements of the RB method are met. Given a tolerance $\varepsilon_{\text{mes}}^{\text{RB}} > 0$ and a finite set of training parameters $\Xi_{\text{mes}}^{\text{RB}} \subset \Omega$ we are ready to run the RB offline stage. The RB approximation of $\mathbf{U}_{\text{EIM}}^{i,x}$ is denoted as $\mathbf{U}_{\text{RB}}^{i,x}$ and the RB approximation of the output of interest $a^{\text{EIM}}(x)$ is defined by

$$a_{ij}^{\text{RB}}(x) = G_{\text{mic}}^i(\mathbf{U}_{\text{RB}}^{j,x}; x) + G_{\text{mic}}^j(\mathbf{U}_{\text{RB}}^{i,x}; x) - A_{\text{mes}}^{\text{EIM}}(\mathbf{U}_{\text{RB}}^{i,x}, \mathbf{U}_{\text{RB}}^{j,x}; x). \quad (96)$$

Macro problem. Finally, we are ready to update the macroscopic problem (49) to the following. Find $p^{H,\text{RB}} \in S^l(\Omega, \mathcal{T}_H)/\mathbb{R}$ such that

$$B_{H,\text{RB}}(p^{H,\text{RB}}, q^H) = L_{H,\text{RB}}(q^H) \quad \forall q^H \in S^l(\Omega, \mathcal{T}_H)/\mathbb{R}, \quad (97)$$

where $B_{H,\text{RB}}$ and $L_{H,\text{RB}}$ are defined as in (50) but with the tensor a^{RB} instead of a^{h_1} .

5.1. Summary. The goal of the method we presented is to solve the macro problem (97), where the permeability a^{RB} needs to be evaluated at every macroscopic quadrature point. Before we can use the RB online computation for a fast evaluation of a^{RB} , several offline algorithms need to run. We plot the processes that yields an online evaluation of a^{RB} in a comprehensive flowchart diagram in Figure 4. For simplicity, we excluded the successive constraint method from the diagram, which needs to be applied twice: before the micro RB offline stage and before the meso RB offline stage.

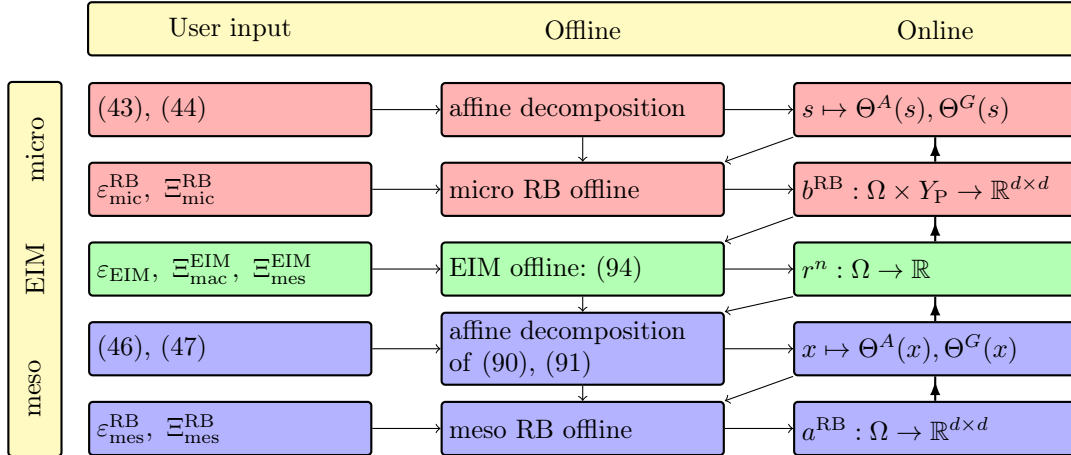


Figure 4: A comprehensive guide to the computation of a^{RB} . Thin arrows show the order of processing. In the “online” column the thick arrows show dependence of computation, for example, to evaluate $b^{\text{RB}}(s)$ for some $s \in \Omega \times Y_{\text{P}}$ we need to evaluate $\Theta^A(s)$ and $\Theta^G(s)$.

Time cost. Let $N_{\text{mic}}^{\text{RB}}$ be the maximal size of the RB on the micro scale (that is, $\max_{i \in \{1, \dots, d\}} N_i$) and let $N_{\text{mes}}^{\text{RB}}$ be the same for the meso scale. Let $N_{\text{mac}}, N_{\text{mes}}, N_{\text{mic}}$ be the number of degrees of freedom of the FE problem (97), (90), (43), respectively. Let $Q_A^{\text{mic}}, Q_G^{\text{mic}}$ and $Q_A^{\text{mes}}, Q_G^{\text{mes}}$ be the sizes of affine decompositions of the micro and the Stokes part of the meso problem, respectively. For simplicity, let us denote $Q_{\text{mic}} = \max\{Q_A^{\text{mic}}, Q_G^{\text{mic}}\}$ and $Q_{\text{mes}} = \max\{Q_A^{\text{mes}}, Q_G^{\text{mes}}\}$.

For any $s \in \Omega \times Y_P$ the time cost of evaluation of $b^{\text{RB}}(s)$ is $\mathcal{O}((N_{\text{mic}}^{\text{RB}} Q_{\text{mic}})^2)$, as was discussed in section 4. For any $x \in \Omega$ the time cost of evaluation of the coefficients $r^n(x)$ for $n = 1, \dots, N_{\text{EIM}}$ takes N_{EIM} online evaluations of b^{RB} and a matrix-vector multiplication with the matrix of size $N_{\text{EIM}} \times N_{\text{EIM}}$, which makes a total of $\mathcal{O}(N_{\text{EIM}}(N_{\text{mic}}^{\text{RB}} Q_{\text{mic}})^2 + N_{\text{EIM}}^2)$. To obtain the time cost of the online evaluation of $a^{\text{RB}}(x)$ we need to add assembling and solution of the online system, which gives $\mathcal{O}(N_{\text{EIM}}(N_{\text{mic}}^{\text{RB}} Q_{\text{mic}})^2 + (N_{\text{mes}}^{\text{RB}}(N_{\text{EIM}} + Q_{\text{mes}}))^2)$ in total. The total time cost of the online stage of the reduced basis three-scale method is thus

$$\mathcal{O}(N_{\text{mac}}(N_{\text{EIM}}(N_{\text{mic}}^{\text{RB}} Q_{\text{mic}})^2 + (N_{\text{mes}}^{\text{RB}}(N_{\text{EIM}} + Q_{\text{mes}}))^2)).$$

5.2. A priori error estimates. In this section we show well-posedness of the RB three-scale numerical method presented and derive a priori error estimates. We follow the a priori error analysis from section 3.2 and take into account the additional approximation techniques: reduced basis and empirical interpolation method.

Let us start with the micro scale. It was shown that the micro problem (33) and its discretization (43) are well-posed (see (40), (42), and (51)). Furthermore, under rather general assumptions on the micro geometries, the permeability tensor b^0 is shown to be uniformly bounded and elliptic (see (20)) and the same is true for b^{h_2} for sufficiently small h_2 (see (56)). Moreover, both b^0 and b^{h_2} are symmetric.

Lemma 14. *Suppose that the assumptions of Lemma 6 hold. Then there exists $C > 0$ such that for any $x \in \Omega \times Y$ we have*

$$\|b^0(s) - b^{\text{RB}}(s)\|_{\text{F}} \leq C \left(h_2^{2(m+1)} + \sum_{i=1}^d \|\mathbf{U}_{h_2}^{i,s} - \mathbf{U}_{\text{RB}}^{i,s}\|_{X_{\text{mic}}}^2 \right).$$

Proof. We use the triangle inequality

$$\|b^0(s) - b^{\text{RB}}(s)\|_{\text{F}} \leq \|b^0(s) - b^{h_2}(s)\|_{\text{F}} + \|b^{h_2}(s) - b^{\text{RB}}(s)\|_{\text{F}}$$

and apply Lemma 6 and the a priori error estimates in output of interest (83). \square

By Lemma 14 and (56) we see that if the error of the RB approximation is sufficiently small, then we can conclude that b^{RB} is also uniformly bounded and constant, that is, there are constants $0 < \lambda_b \leq \Lambda_b$ (denoted similarly as in (20), for simplicity) such that

$$b^{\text{RB}}(s)\xi \cdot \xi \geq \lambda_b |\xi|^2, \quad |b^{\text{RB}}(s)\xi| \leq \Lambda_b |\xi|, \quad \forall \xi \in \mathbb{R}^d, \forall s \in \Omega \times Y. \quad (98)$$

Furthermore, by symmetry of A_{mic} , the tensor b^{RB} is also symmetric.

Similarly as in section 3.2 we conclude from (98) and (6) that $\beta^{\text{RB}}(s)$ is bounded, and positive definite, that is, there are constants $0 < \lambda_K \leq \Lambda_K$ (denoted the same as in (21), for simplicity of notation) such that

$$\beta^{\text{RB}}(x, y)\xi \cdot \xi \geq \lambda_K |\xi|^2, \quad |\beta^{\text{RB}}(x, y)\xi| \leq \Lambda_K |\xi|, \quad \forall \xi \in \mathbb{R}^d, \forall (x, y) \in \Omega \times Y_P. \quad (99)$$

Since b^{RB} is symmetric then $\beta^{\text{RB}}(s)$ is symmetric too. Furthermore, there is a constant $C > 0$ that depends only on λ_K and Λ_K such that

$$\|\beta^{h_2}(s) - \beta^{\text{RB}}(s)\|_{\text{F}} \leq C \|b^{h_2}(s) - b^{\text{RB}}(s)\|_{\text{F}} \quad \forall s \in \Omega \times Y_P.$$

Finally, consider the EIM approximation of β^{RB} that we denoted by β^{EIM} and defined in (94). The bound (95) is a priori valid only on the EIM training set. Assuming that (95) is valid for all $(x, y) \in \Omega \times Q^{h_1}$, it can be derived from (99) that β^{EIM} is also uniformly elliptic and bounded for a sufficiently small tolerance ε_{EIM} . Hence, there are constants $0 < \lambda_K \leq \Lambda_K$ (using the same notation as in (21), for simplicity) such that

$$\beta^{\text{EIM}}(x, y)\xi \cdot \xi \geq \lambda_K |\xi|^2, \quad |\beta^{\text{EIM}}(x, y)\xi| \leq \Lambda_K |\xi|, \quad \forall \xi \in \mathbb{R}^d, \forall (x, y) \in \Omega \times Q^{h_1}.$$

Consequently, the meso problem (90) is well-posed, that is, there are constants $0 < \lambda_{\text{mes}} \leq \Lambda_{\text{mes}}$ (using the same notation as in (41), for simplicity) such that for any $x \in \Omega$ we have

$$\inf_{\substack{\mathbf{U} \in X_{\text{mes}}^{h_1} \\ \mathbf{U} \neq 0}} \sup_{\substack{\mathbf{V} \in X_{\text{mes}}^{h_1} \\ \mathbf{V} \neq 0}} \frac{A_{\text{mes}}^{\text{EIM}}(\mathbf{U}, \mathbf{V}; x)}{\|\mathbf{U}\|_{X_{\text{mes}}} \|\mathbf{V}\|_{X_{\text{mes}}}} \geq \lambda_{\text{mes}}, \quad \sup_{\substack{\mathbf{U} \in X_{\text{mes}}^{h_1} \\ \mathbf{U} \neq 0}} \sup_{\substack{\mathbf{V} \in X_{\text{mes}}^{h_1} \\ \mathbf{V} \neq 0}} \frac{A_{\text{mes}}^{\text{EIM}}(\mathbf{U}, \mathbf{V}; x)}{\|\mathbf{U}\|_{X_{\text{mes}}} \|\mathbf{V}\|_{X_{\text{mes}}}} \leq \Lambda_{\text{mes}}. \quad (100)$$

Hence, the RB method at the meso scale is also well-posed and the macroscopic permeability $a^{\text{RB}}(x)$ is well-defined in (96). Since β^{EIM} is symmetric it is evident that $A_{\text{mic}}^{\text{EIM}}$ is symmetric and thus a^{RB} is symmetric.

Lemma 15. *Suppose that (100) and the assumptions from Lemma 7 hold. Then there is $C > 0$ such that for any $x \in \Omega$ we have*

$$\|a^0(x) - a^{\text{RB}}(x)\|_{\text{F}} \leq C \left(h_1^{2(k+1)} + \max_{y \in Q^{h_1}} \|\beta^0(x, y) - \beta^{\text{EIM}}(x, y)\|_{\text{F}} + \sum_{i=1}^d \|\mathbf{U}_{\text{EIM}}^{i,x} - \mathbf{U}_{\text{RB}}^{i,x}\|_{X_{\text{mes}}}^2 \right).$$

Proof. The triangle inequality gives

$$\|a^0(x) - a^{\text{RB}}(x)\|_{\text{F}} \leq \|a^0(x) - a^{\text{EIM}}(x)\|_{\text{F}} + \|a^{\text{EIM}}(x) - a^{\text{RB}}(x)\|_{\text{F}}.$$

Using Lemma 7 for the first term and the a priori error estimates in output of interest (83) for the second term gives the desired result. \square

For sufficiently good RB and EIM approximation and sufficiently small h_2 and h_1 we get that a^{RB} is uniformly elliptic and bounded. Thus, there are constants $0 < \lambda_a \leq \Lambda_a$ (denoted as in (27), for simplicity) such that

$$a^{\text{RB}}(x)\xi \cdot \xi \geq \lambda_a |\xi|^2, \quad |a^{\text{RB}}(x)\xi| \leq \Lambda_a |\xi|, \quad \forall \xi \in \mathbb{R}^d, \quad \forall x \in \Omega. \quad (101)$$

This leads to the first global a priori error estimate.

Lemma 16. *Suppose that (101) and the assumptions of Lemma 8 hold. Then there is $C > 0$ such that*

$$|p^0 - p^{H,\text{RB}}|_{H^1(\Omega)} \leq C \left(H^l + \|\mathbf{f} - \mathbf{f}^H\|_{L^2(\Omega)^d} + \|\mathbf{f}^H\|_{L^2(\Omega)^d} \max_{x \in Q^H} \|a^0(x) - a^{\text{RB}}(x)\|_{\text{F}} \right).$$

Proof. The proof follows the a priori error analysis from [1, Section 4]. \square

Finally, we propose a fully discrete a priori error estimate.

Theorem 17. *Suppose that assumptions of Lemma 16, Lemma 15, and Lemma 14 hold and that $\mathbf{f} \in H^l(\Omega)^d$. Then there is a constant $C > 0$ such that*

$$\begin{aligned} |p^0 - p^{H,\text{RB}}|_{H^1(\Omega)} \leq C & \left(H^l + h_1^{2(k+1)} + h_2^{2(m+1)} + \max_{s \in Q^H \times Q^{h_1}} \sum_{i=1}^d \|\mathbf{U}_{h_2}^{i,s} - \mathbf{U}_{\text{RB}}^{i,s}\|_{X_{\text{mic}}}^2 \right. \\ & \left. + \max_{s \in Q^H \times Q^{h_1}} \|\beta^{\text{RB}}(s) - \beta^{\text{EIM}}(s)\|_{\text{F}} + \max_{x \in Q^H} \sum_{i=1}^d \|\mathbf{U}_{\text{EIM}}^{i,x} - \mathbf{U}_{\text{RB}}^{i,x}\|_{X_{\text{mes}}}^2 \right). \end{aligned}$$

Proof. The proof is a direct application of Lemma 16, Lemma 15, and Lemma 14. The regularity of \mathbf{f} allows the estimate $\|\mathbf{f} - \mathbf{f}^H\|_{L^2(\Omega)^d} \leq CH^l$. \square

In Theorem 17 we resolved the errors coming from the FE discretization of the macro, meso, and micro problems but we left the error terms stemming from the RB and EIM. If the training sets of the offline algorithms include all the quadrature points, we get an estimate

$$|p^0 - p^{H,\text{RB}}|_{H^1(\Omega)} \leq C \left(N_{\text{mac}}^{-\frac{l}{d}} + N_{\text{mes}}^{-\frac{2(k+1)}{d}} + N_{\text{mic}}^{-\frac{2(m+1)}{d}} + (\varepsilon_{\text{mes}}^{\text{RB}})^2 + \varepsilon_{\text{EIM}} + (\varepsilon_{\text{mic}}^{\text{RB}})^2 \right), \quad (102)$$

where we used the degrees of freedom instead of mesh sizes as in (71). Let us remind that in the online stage of the reduced basis three-scale method we can only change the macroscopic mesh (H or N_{mac}) and the number of RB functions used at the meso scale, where we are limited from above by the maximum achieved in the offline stage. All the other parameters in Theorem 17 or in (102) have to be fixed in the offline stage. If the Kolmogorov n -widths of the mesoscopic and microscopic solution manifolds decay exponentially, then so are the mesoscopic and microscopic RB errors.

6 Numerical experiments.

In this section we test the proposed reduced basis three-scale method and study the effect of different parameter choices on the global error.

Implementation. All experiments were performed on a single computer with two 8-core processors Intel Xeon E5-2600 and 64 GB of RAM with Matlab R2015b. The finite element code is inspired by [5, 15] and it uses vectorization techniques to achieve fast assembling. Sparse linear systems are solved by the Matlab routine `mldivide`. Linear systems with the same positive definite matrix representing the inner product on X_h are solved repeatedly in the offline algorithms. We optimize this by precomputing a sparse Cholesky factorization (Matlab routine `chol`). Generalized eigenproblems from the SCM method were solved using the Matlab package `bleigifp` [23], which implements a block, inverse-free Krylov subspace method. Linear programming problems from the SCM method are solved by the Matlab routine `linprog` with the default settings.

Macro scale. We consider the macroscopic domain $\Omega = (0, 2) \times (0, 3)$ with periodic boundary between the bottom edge $(0, 2) \times \{0\}$ and the top edge $(0, 2) \times \{3\}$ and Neumann boundary conditions elsewhere. The macroscopic force field is constant $\mathbf{f} \equiv (0, -1)$. The macro geometry and the coarsest macroscopic mesh are both shown in Figure 5.

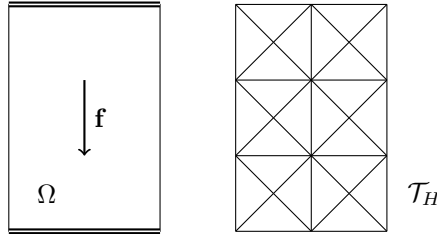


Figure 5: Macroscopic domain Ω with the direction of the constant force field \mathbf{f} (left) and the coarsest macroscopic mesh \mathcal{T}_H that we consider (right).

Meso scale. To describe the porosity at the meso scale we define the reference meso geometry (Y_F, Y_P) and the mapping φ_{mes} . Let

$$Y_P = \{y \in Y; \max\{|y_1|, |y_2|\} < 1/8 \text{ or } |y_1| > 3/8 \text{ or } |y_2| > 3/8\}$$

as is depicted in Figure 6. The fluid part is then the complement $Y_F = Y \setminus Y_P$. We define φ_{mes} implicitly by describing the local mesoscopic domains $Y_P^x = \varphi_{\text{mes}}(x, Y_P)$ and $Y_F^x = \varphi_{\text{mes}}(x, Y_F)$. For any $x \in \Omega$ let Y_P^x be such that the outer layer is unchanged but the inner square is moved so that it is centered at the point with coordinates $[\mu_1(x), \mu_2(x)]$, where

$$\begin{aligned} \mu_1(x) &= \frac{1}{8} \sin\left(\frac{\pi x_1}{2} + \frac{2\pi x_2}{3}\right), \\ \mu_2(x) &= \frac{1}{8} \sin\left(\frac{\pi x_1}{2} - \frac{2\pi x_2}{3}\right). \end{aligned}$$

The mesoscopic domain Y can be divided into 6 subdomains as is shown in Figure 6 and the deformation $\varphi_{\text{mes}}(x, \cdot) : Y \rightarrow Y$ can be defined so that it is affine in each of these subdomains. It is important that $|\mu_1(x)| < 1/4$ and $|\mu_2(x)| < 1/4$ so that this deformation is not degenerate.

Micro scale. To describe the porosity at the micro scale we define the reference micro geometry (Z_F, Z_S) and the mapping φ_{mic} . We define Z_F and the coarsest micro mesh \mathcal{T}_{h_2} as is depicted in Figure 7. We define φ_{mic} implicitly by describing the local microscopic domain $Z_F^s = \varphi_{\text{mic}}(s, Z_F)$. It is shown in Figure 7 how Z_F can be divided by two horizontal and two vertical lines. For any $s = (x, y) \in \Omega \times Y$ the fluid part Z_F^s can be obtained by simply moving these lines so that the geometry is stretched or contracted in the directions z_1 and z_2 as is

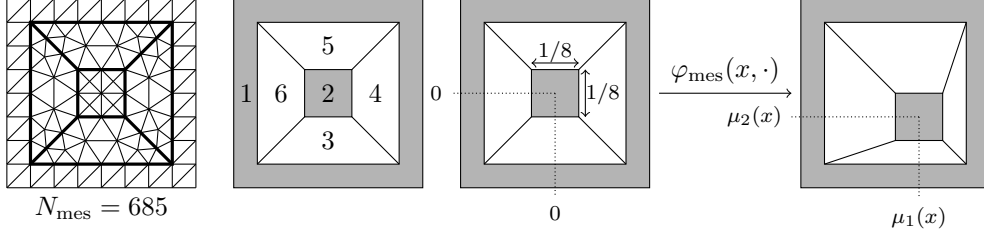


Figure 6: From left to right: the coarsest mesoscopic mesh \mathcal{T}_{h_1} ; division of Y into six regions such that φ_{mes} is affine in each of them; reference mesoscopic domain (Y_P, Y_F) ; local mesoscopic domain (Y_P^x, Y_F^x) that is obtained by applying φ_{mes} .

shown in Figure 7, where the deformation is controlled by

$$\begin{aligned}\mu_1(x, y) &= \frac{1}{12} \sin\left(\frac{\pi x_1}{2} - \frac{2\pi x_2}{3}\right) \cos(2\pi y_2), \\ \mu_2(x, y) &= \frac{1}{12} \sin\left(\frac{\pi x_1}{2} - \frac{2\pi x_2}{3} + 2\pi y_1 + 2\pi y_2\right).\end{aligned}\tag{103}$$

Hence, Z_F can be divided into 8 regions such that $\varphi_{\text{mic}}(s, \cdot)$ is affine in each region.

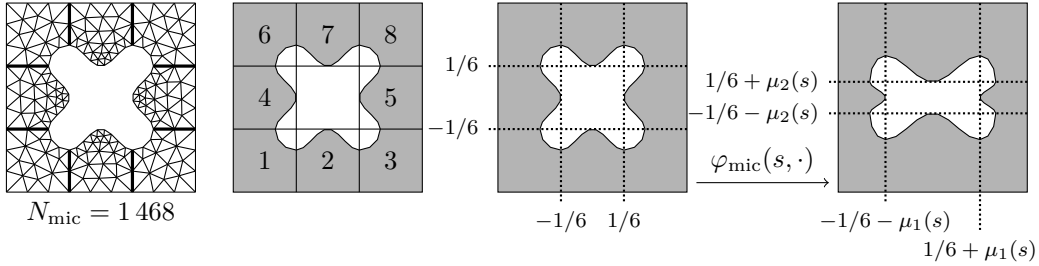


Figure 7: From left to right: the coarsest microscopic mesh \mathcal{T}_{h_1} ; division of Y into eight regions such that φ_{mic} is affine in each of them; reference microscopic domain (Z_F, Z_S) ; local microscopic domain (Z_F^s, Z_S^s) that is obtained by applying φ_{mic} .

Fine scale solution. For an illustration of the three-scale porous media that we just defined, we plot in Figure 8 the solution $p^{\varepsilon_1, \varepsilon_2}$ to the fine-scale problem (9) with $\varepsilon_1 = 1/4$ and $\varepsilon_2 = 1/32$. This solution was obtained numerically using a mesh with 908 252 nodes, which yielded 7 777 418 DOF with $\mathcal{P}^2/\mathcal{P}^1$ finite elements.

Offline computation. We now provide a step by step description of the application of the reduced basis three-scale method to a test problem. We describe the choice of the various parameters and illustrate how they influence the error.

The offline part of the three-scale method is performed in the bottom-up manner, starting with the micro scale. The microscopic geometry is described in Figure 7 and its parametrization is given in (103). The coarsest micro mesh that we consider is in Figure 7(left) and using $\mathcal{P}^2/\mathcal{P}^1$ finite elements gives $N_{\text{mic}} = 1468$. Using the technique from [4] we created refined micro meshes depicted in Figure 9.

To apply the RB method at the micro scale we need an affine decomposition of the micro problem. Since the deformation function φ_{mic} satisfies Assumption 11 such a decomposition is available via (86). We can symbolically reduce this decomposition to size $Q_A = 12$ and $Q_G = 4$. The same random sample of parameters $\Xi_{\text{mic}}^{\text{SCM}} = \Xi_{\text{mic}}^{\text{RB}} \subset \Omega \times Y$ was selected for both offline SCM and RB algorithms. The sample size was set to 128^2 and the offline SCM stage was executed with $\varepsilon_{\text{SCM}} = \theta = 0.5$. Instead of a tolerance for the a posteriori error estimator, we stopped the offline RB stage (Algorithm 10) when we reached the number of RB functions equal to 50. In the experiments we will then vary the size of the RB denoted by $N_1 = N_2 = N_{\text{mic}}^{\text{RB}} \leq 50$.

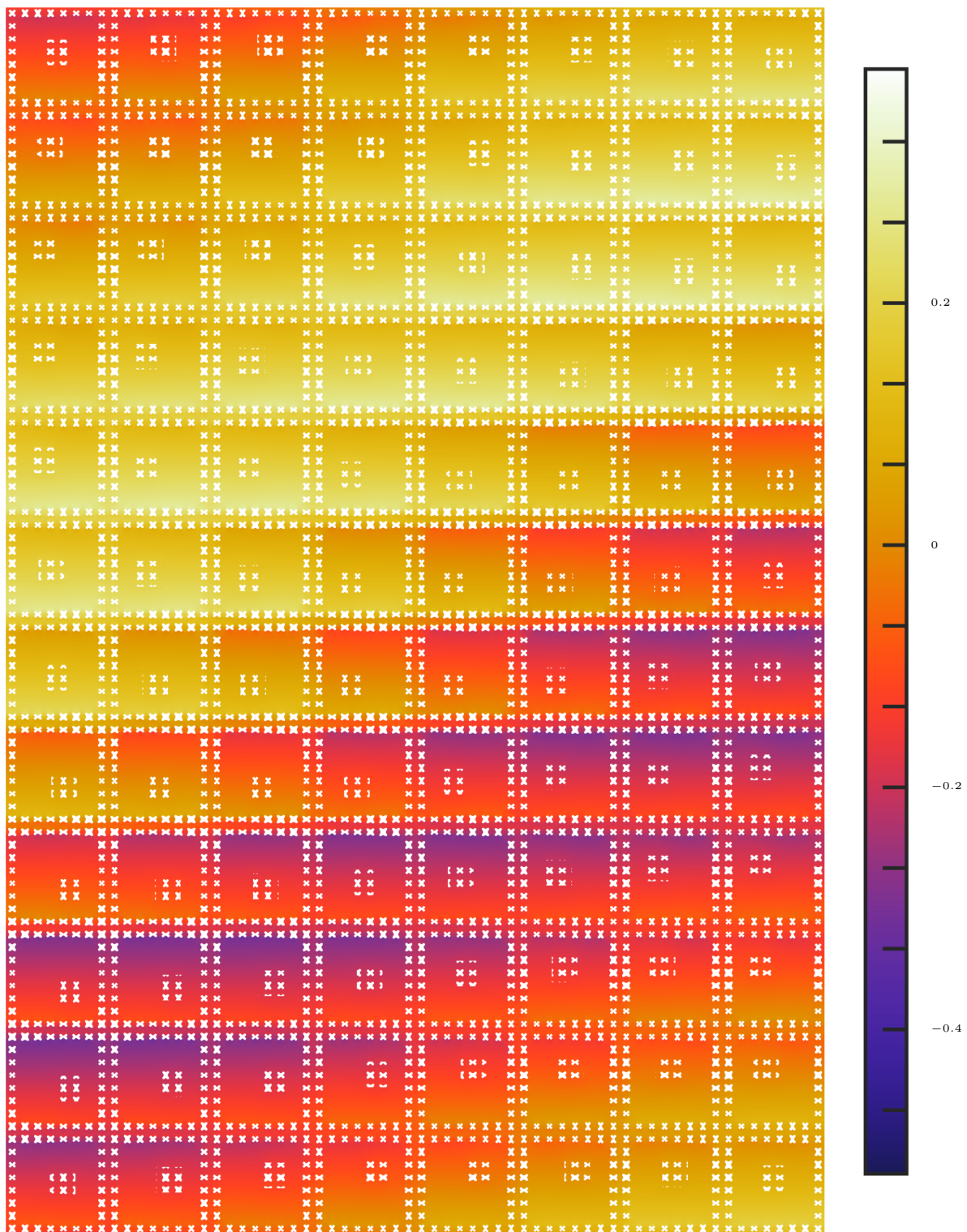


Figure 8: A solution $p^{\varepsilon_1, \varepsilon_2}$ to the fine-scale problem (9) with $\varepsilon_1 = 1/4$ and $\varepsilon_2 = 1/32$.

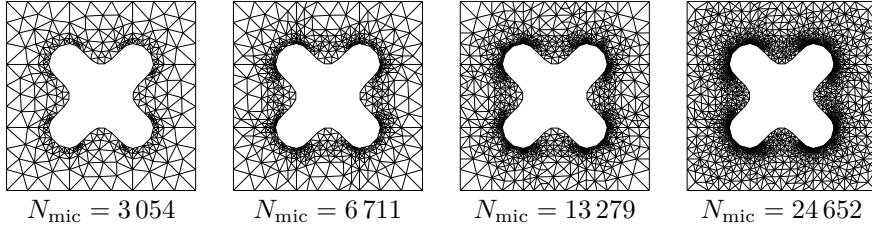


Figure 9: Graded microscopic meshes and the corresponding number of DOF of the micro problems when discretized with $\mathcal{P}^2/\mathcal{P}^1$ FE.

Having completed the offline stage on the micro scale, we now have a fast online evaluation of $b^{\text{RB}}(s)$ for any $s \in \Omega \times Y$ and we continue with the meso scale offline computation. The mesoscopic geometry deformation and the coarsest meso mesh are depicted in Figure 6. We will consider also finer meso meshes that are obtained via uniform refinement and shown in Figure 10.

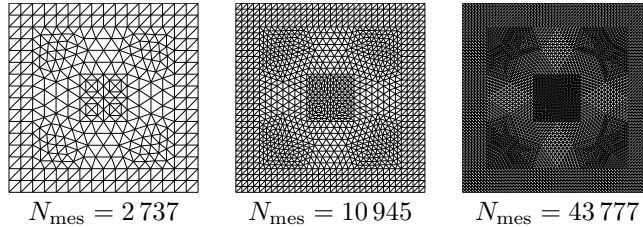


Figure 10: Uniformly refined meso meshes and the corresponding number of DOF of the micro problems when discretized with $\mathcal{P}^2/\mathcal{P}^1$ FE.

Affine decomposition of the meso scale is achieved by two means, as described in section 5. We consider the modified meso problem (90) with the bilinear form $A_{\text{mes}}^{\text{EIM}}$ defined in (89) and the linear form G_{mes}^i . The first part of A_{mes} (denoted by $A_{\text{mes}}^{\text{stokes}}$) and G_{mes}^i give an affine decomposition as in the micro scale because the meso geometry deformation φ_{mes} satisfies Assumption 12. The second part of A_{mes} (see (89)) comes from the EIM applied to β^{RB} as shown in (94). In the offline EIM stage (Algorithm 13) we select random training sets $\Xi_{\text{mac}}^{\text{EIM}} \subset \Omega$ and $\Xi_{\text{mes}}^{\text{EIM}} \subset Q^{h_1}$ of size at most 4096. We repeat the offline EIM cycle for 100 iterations and in what follows we denote by N_{EIM} the size of the EIM basis that we use ($N_{\text{EIM}} \leq 100$). The size of the meso affine decomposition is then $Q_A = 16 + N_{\text{EIM}}$ and $Q_F = 4$.

With an affine decomposition of the meso problem (90) we can continue with the RB offline computation (Algorithm 10) at the meso scale. Since the variation of the inf-sup constant is minimal, we used a constant estimate instead of the SCM algorithm. A random sample of parameters $\Xi_{\text{mes}}^{\text{RB}} \subset \Omega$ was selected with sample size 128^2 . We performed the offline greedy algorithm until we reached the number of RB functions equal to 50. In the experiments we will then vary the size of the RB denoted by $N_1 = N_2 = N_{\text{mes}}^{\text{RB}} \leq 50$.

Let us remark that the micro mesh, micro RB size, meso mesh, and the size of the EIM are fixed in the offline stage and can be changed only by running the offline stage again. The size of the meso RB (not exceeding the maximal size that was computed in the meso RB offline stage) and the macroscopic discretization can be freely changed in the online stage.

Reference solution. We are not aware of any three-scale locally periodic porous media with an explicitly known macro solution p^0 or tensors a^0 or b^0 in a closed form. Thus, whenever we compare to p^0 in numerical experiments, we use a fine numerical approximation of p^0 . This reference solution is obtained by the reduced basis three-scale numerical method with the parameters described in Table 3.

Numerical tests. In the online stage we used macroscopic mesh from Figure 5 and its uniform refinements. We tested \mathcal{P}^1 , \mathcal{P}^2 , and \mathcal{P}^3 macroscopic FE but in the experiments

| | | | |
|------------------|-----------------------------|----------|-------------------------------|
| micro mesh (DOF) | $N_{\text{mic}} = 212\,267$ | micro FE | $\mathcal{P}^2/\mathcal{P}^1$ |
| micro RB size | $N_1 = N_2 = 50$ | | |
| EIM size | $N_{\text{EIM}} = 100$ | | |
| meso mesh (DOF) | $N_{\text{mes}} = 700\,417$ | meso FE | $\mathcal{P}^2/\mathcal{P}^1$ |
| meso RB size | $N_1 = N_2 = 50$ | | |
| macro mesh (DOF) | $N_{\text{mac}} = 442\,944$ | macro FE | \mathcal{P}^3 |

Table 3: Parameters of the three-scale reference solution.

below we show only results with \mathcal{P}^2 and \mathcal{P}^3 to monitor the saturation of the error with micro and meso parameter variation.

In Table 4 we define micro and meso parameters of a solution that will be taken as the starting point of the following experiments. Each time we will vary one of the parameters and see how it influences the macroscopic error with \mathcal{P}^2 and \mathcal{P}^3 macroscopic FE. In all the experiments we observe (see Figures 11–15) that the macroscopic error converges as $N_{\text{mac}}^{-1/d}$ when the meso and micro errors are negligible. For larger values of N_{mac} the macro error saturates and this saturation level depends on the varying parameter. This corroborates the a priori error estimate of Theorem 17.

| | | | |
|------------------|----------------------------|----------|-------------------------------|
| micro mesh (DOF) | $N_{\text{mic}} = 24\,654$ | micro FE | $\mathcal{P}^2/\mathcal{P}^1$ |
| micro RB size | $N_1 = N_2 = 20$ | | |
| EIM size | $N_{\text{EIM}} = 50$ | | |
| meso mesh (DOF) | $N_{\text{mes}} = 43\,777$ | meso FE | $\mathcal{P}^2/\mathcal{P}^1$ |
| meso RB size | $N_1 = N_2 = 20$ | | |

Table 4: Micro and meso parameters of the most precise RB solution considered.

In Figure 11 we show how the micro mesh influences the accuracy of the three-scale method. All the parameters from Table 4 are fixed except the micro mesh (N_{mic}), which varies over the meshes from Figure 7(left) and Figure 9. The following experiments are of similar nature.

In Figure 12 we show how the size of the micro RB influences the accuracy of the method. All the parameters from Table 4 are fixed except for the micro RB size $N_{\text{mic}}^{\text{RB}}$ that varies over values $\{4, 8, 12, 16, 20\}$.

Let us now discuss the effects of changing the mesoscopic parameters. The influence of the mesoscopic mesh is shown in Figure 13. We select the meso meshes from Figure 6(left) and Figure 10 while the other parameters from Table 4 are fixed.

The influence of the size of the EIM for β^{RB} used at the meso scale is depicted in Figure 14. The parameter N_{EIM} is chosen from the set $\{10, 20, 30, 40, 50\}$.

Finally, the effect of the size of the meso RB size is depicted in Figure 15, where $N_{\text{mes}}^{\text{RB}}$ are chosen from $\{4, 8, 12, 16, 20\}$.

These five experiments shows that the error is influenced by all parameters and they should be carefully selected to achieve good accuracy and performance. Moreover, except the size of the meso RB that we use, all the other parameters have to be fixed in the offline stage of the three-scale method.

References

- [1] ABDULLE, A., AND BUDÁČ, O. An adaptive finite element heterogeneous multiscale method for Stokes flow in porous media. *Multiscale Model. Simul.* 13 (2015), 256–290.
- [2] ABDULLE, A., AND BUDÁČ, O. A discontinuous Galerkin reduced basis numerical homogenization method for fluid flow in porous media. submitted to SIAM J. Sci. Comput., 2015.
- [3] ABDULLE, A., AND BUDÁČ, O. A Petrov–Galerkin reduced basis approximation of the Stokes equation in parameterized geometries. *C. R. Math. Acad. Sci. Paris* 353, 7 (2015), 641–645.

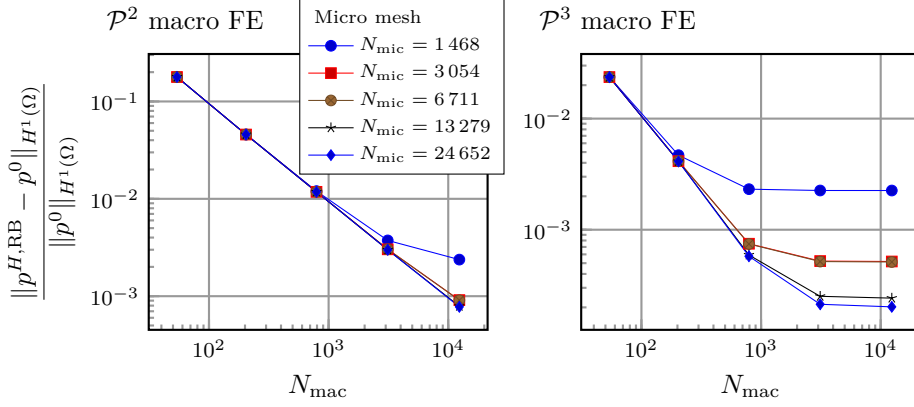


Figure 11: Error saturation with respect to the micro mesh variation.

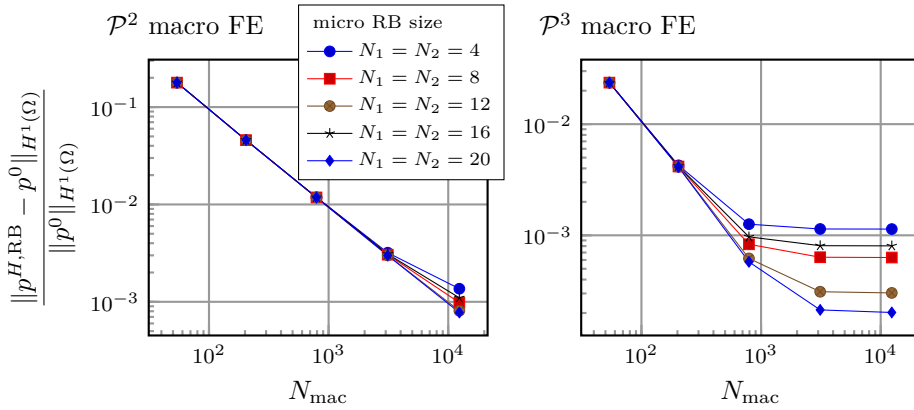


Figure 12: Error saturation with respect to variation of the micro RB size.

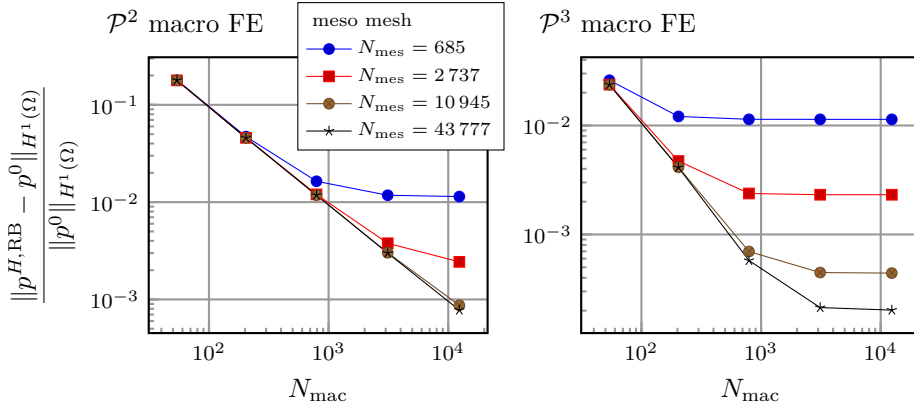


Figure 13: Error saturation with respect to the meso mesh variation.

- [4] ABDULLE, A., AND BUDÁČ, O. A reduced basis finite element heterogeneous multiscale method for Stokes flow in porous media. accepted in *Comp. Meth. Appl. Mech. Eng.*, 2015.
- [5] ABDULLE, A., AND NONNENMACHER, A. A short and versatile finite element multiscale code for homogenization problems. *Comput. Methods Appl. Mech. Engrg.* 198, 37–40 (2009), 2839–2859.
- [6] ALLAIRE, G. Homogenization of the Stokes flow in a connected porous medium. *Asymptot. Anal.* 2, 3 (1989), 203–222.
- [7] ALYAEV, S., KEILEGAVLEN, E., AND NORDBOTTEN, J. M. Analysis of control volume

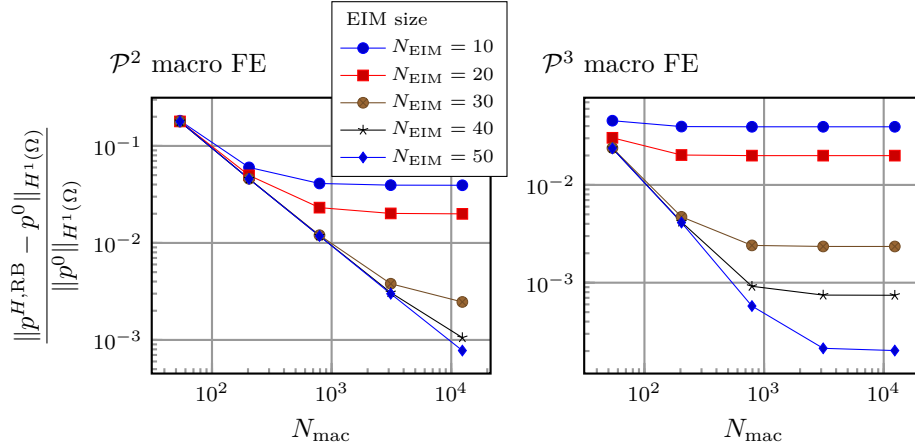


Figure 14: Error saturation with respect to EIM size variation.

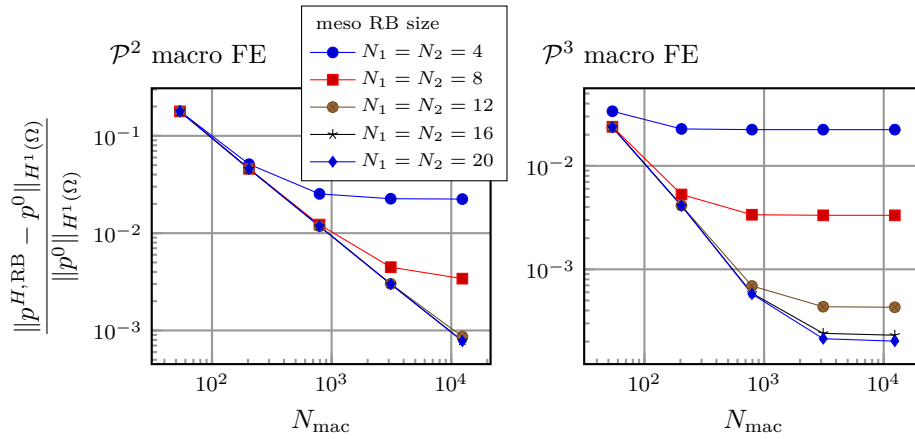


Figure 15: Error saturation with respect to variation of the meso RB size.

heterogeneous multiscale methods for single phase flow in porous media. *Multiscale Model. Simul.* 12, 1 (2014), 335–363.

- [8] BARRAULT, M., MADAY, Y., NGUYEN, N.-C., AND PATERA, A. T. An ‘empirical interpolation method’: Application to efficient reduced-basis discretization of partial differential equations. *C. R. Math. Acad. Sci. Paris Ser. I* 339 (2004), 667–672.
- [9] BEAVERS, G. S., AND JOSEPH, D. D. Boundary conditions at a naturally permeable wall. *Journal of fluid mechanics* 30, 01 (1967), 197–207.
- [10] BELIAEV, A. Y., AND KOZLOV, S. M. Darcy equation for random porous media. *Comm. Pure Appl. Math.* 49, 1 (1996), 1–34.
- [11] BINEV, P., COHEN, A., DAHMEN, W., DEVORE, R., PETROVA, G., AND WOJTASZCZYK, P. Convergence rates for greedy algorithms in reduced basis methods. *SIAM J. Math. Anal.* 43 (2011), 1457–1472.
- [12] BROWN, D. L., EFENDIEV, Y., AND HOANG, V. H. An efficient hierarchical multiscale finite element method for Stokes equations in slowly varying media. *Multiscale Model. Simul.* 11, 1 (2013), 30–58.
- [13] BROWN, D. L., POPOV, P., AND EFENDIEV, Y. On homogenization of Stokes flow in slowly varying media with applications to fluid-structure interaction. *GEM Int. J. Geomath.* 2, 2 (2011), 281–305.
- [14] BUDÁČ, O. *Multiscale methods for Stokes flow in heterogeneous media*. PhD thesis, École Polytechnique Fédérale de Lausanne, Lausanne, 2016.
- [15] CHEN, L., AND ZHANG, C.-S. AFEM@Matlab: a matlab package of adaptive finite element methods. Tech. rep., Department of Mathematics, University of Maryland at

- College Park, 2006.
- [16] CIARLET, P. G. *The finite element method for elliptic problems.*, vol. 40 of *Classics Appl. Math.* SIAM, Philadelphia, 2002.
 - [17] CIARLET, P. G., AND RAVIART, P. A. The combined effect of curved boundaries and numerical integration in isoparametric finite element methods. In *The mathematical foundations of the finite element method with applications to partial differential equations* (1972), pp. 409–474.
 - [18] DARCY, H. Les fontaines publiques de la ville de Dijon: Exposition et application à suivre et des formules à employer dans les questions de distribution d'eau, 1856.
 - [19] GRIEBEL, M., AND KLITZ, M. Homogenization and numerical simulation of flow in geometries with textile microstructures. *Multiscale Model. Simul.* 8, 4 (2010), 1439–1460.
 - [20] HUYNH, D. B. P., KNEZEVIC, D. J., CHEN, Y., HESTHAVEN, J. S., AND PATERA, A. T. A natural-norm successive constraint method for inf-sup lower bounds. *Comput. Methods Appl. Mech. Engrg.* 199, 29 (2010), 1963–1975.
 - [21] MIKELIC, A., AND JÄGER, W. On the interface boundary condition of Beavers, Joseph, and Saffman. *SIAM Journal on Applied Mathematics* 60, 4 (2000), 1111–1127.
 - [22] PIERCE, N. A., AND GILES, M. B. Adjoint recovery of superconvergent functionals from PDE approximations. *SIAM Rev.* 42, 2 (2000), 247–264.
 - [23] QUILLEN, P. D. *Generalizations of an inverse free Krylov subspace method for the symmetric generalized eigenvalue problem.* PhD thesis, University of Kentucky, 2005.
 - [24] ROVAS, D. V. *Reduced-basis output bound methods for parametrized partial differential equations.* PhD thesis, Massachusetts Institute of Technology, 2003.
 - [25] ROZZA, G., HUYNH, D. B. P., AND MANZONI, A. Reduced basis approximation and a posteriori error estimation for Stokes flows in parametrized geometries: roles of the inf-sup stability constants. *Numer. Math.* 125, 1 (2013), 1–38.
 - [26] SAFFMAN, P. G. On the boundary condition at the surface of a porous medium. *Studies in Applied Mathematics* 50, 2 (1971), 93–101.
 - [27] SÁNCHEZ-PALENCIA, E. *Non-homogeneous media and vibration theory*, vol. 127 of *Lecture Notes in Phys.* Springer, 1980.
 - [28] TARTAR, L. *Incompressible fluid flow in a porous medium—convergence of the homogenization process.* Vol. 127 of *Lecture Notes in Phys.* [27], 1979, ch. Appendix, pp. 368–377.

Recent publications:

MATHEMATICS INSTITUTE OF COMPUTATIONAL SCIENCE AND ENGINEERING

Section of Mathematics

Ecole Polytechnique Fédérale (EPFL)

CH-1015 Lausanne

- 17.2016** ANDREA MANZONI, LUCA PONTI :
An adjoint-based method for the numerical approximation of shape optimization problems in presence of fluid-structure interaction
- 18.2016** STEFANO PAGANI, ANDREA MANZONI, ALFIO QUARTERONI:
A reduced basis ensemble Kalman filter for state/parameter identification in large-scale nonlinear dynamical systems
- 19.2016** ANDREA MANZONI, FEDERICO NEGRI :
Automatic reduction of PDEs defined on domains with variable shape
- 20.2016** MARCO FEDELE, ELENA FAGGIANO, LUCA DEDÈ, ALFIO QUARTERONI:
A patient-specific aortic valve model based on moving resistive immersed implicit surfaces
- 21.2016** DIANA BONOMI, ANDREA MANZONI, ALFIO QUARTERONI:
A matrix discrete empirical interpolation method for the efficient model reduction of parametrized nonlinear PDEs: application to nonlinear elasticity problems
- 22.2016** JONAS BALLANI, DANIEL KRESSNER, MICHAEL PETERS:
Multilevel tensor approximation of PDEs with random data
- 23.2016** DANIEL KRESSNER, ROBERT LUCE:
Fast computation of the matrix exponential for a Toeplitz matrix
- 24.2016** FRANCESCA BONIZZONI, FABIO NOBILE, ILARIA PERUGIA:
Convergence analysis of Padé approximations for Helmholtz frequency response problems
- 25.2016** MICHELE PISARONI, FABIO NOBILE, PÉNÉLOPE LEYLAND:
A continuation multi level Monte Carlo (C-MLMC) method for uncertainty quantification in compressible aerodynamics
- 26.2016** ASSYR ABDULLE, ONDREJ BUDÁČ:
Multiscale model reduction methods for flow in heterogeneous porous media
- 27.2016** ASSYR ABDULLE, PATRICK HENNING:
Multiscale methods for wave problems in heterogeneous media
- 28.2016** ASSYR ABDULLE, ORANE JECKER:
On heterogeneous coupling of multiscale methods for problems with and without scale separation
- 29.2016** WOLFGANG HACKBUSCH, DANIEL KRESSNER, ANDRÉ USCHMAJEW:
Perturbation of higher-order singular values
- 30.2016** ASSYR ABDULLE, ONDREJ BUDÁČ, ANTOINE IMBODEN:
Multiscale methods and model order reduction for flow problems in three-scale porous media